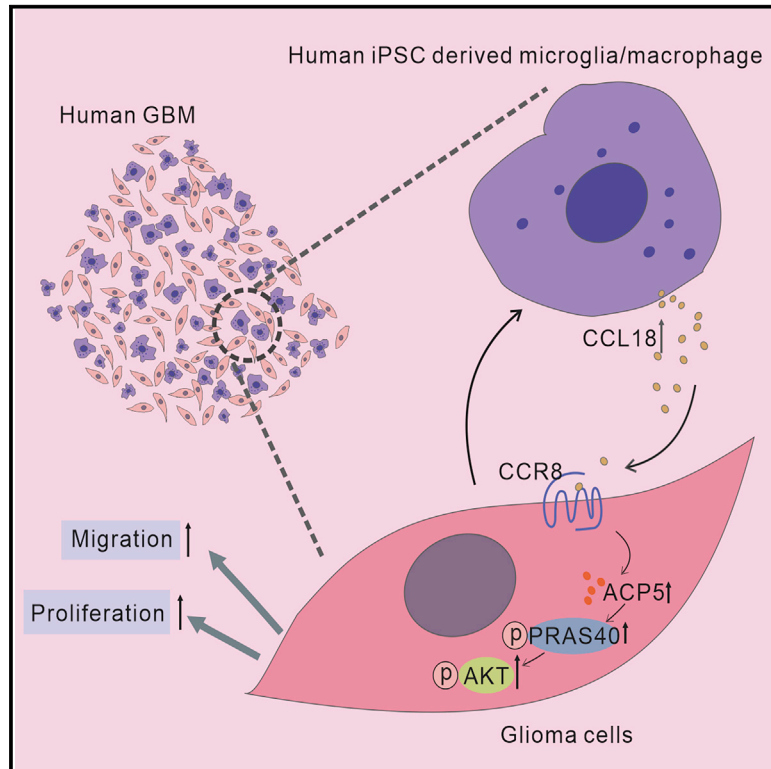


# Microglia/macrophage-derived human CCL18 promotes glioma progression via CCR8-ACP5 axis analyzed in humanized slice model

## Graphical abstract



## Authors

Yimin Huang, Edyta Motta, Cynthia Nanvuma, ..., Michael Synowitz, Charlotte Flüh, Helmut Kettenmann

## Correspondence

charlotte.flueh@uksh.de (C.F.),  
kettenmann@mdc-berlin.de (H.K.)

## In brief

Huang et al. developed an *ex vivo* model by transplanting induced pluripotent stem cell (iPSC)-derived human microglia (iMGL) to investigate the effect of human microglia/macrophage-derived CCL18 on glioma cells. They show that CCL18 promotes glioma cell proliferation and migration via ACP5/PRAS40/Akt signaling.

## Highlights

- Transplanting iPSC-derived human microglia and glioma cells into murine brain slices
- CCL18 expressed by glioma-associated microglia/macrophages promotes glioma cell growth
- CCR8 acts as functional receptor for the CCL18-induced tumor-promoting effect
- CCL18 promotes glioma progression via ACP5/PRAS40/Akt signaling cascade



## Article

# Microglia/macrophage-derived human CCL18 promotes glioma progression via CCR8-ACP5 axis analyzed in humanized slice model

Yimin Huang,<sup>1,2,3</sup> Edyta Motta,<sup>1</sup> Cynthia Nanvuma,<sup>1,4</sup> Leonard D. Kuhrt,<sup>1,2</sup> Yang Yuan,<sup>1</sup> Pengfei Xia,<sup>1</sup> Malgorzata Lubas,<sup>1</sup> Shuai Zhu,<sup>1</sup> Marina Schnauss,<sup>1</sup> Niyeti Qazi,<sup>1</sup> Feng Hu,<sup>3</sup> Huaqiu Zhang,<sup>3</sup> Ting Lei,<sup>3</sup> Michael Synowitz,<sup>4</sup> Charlotte Flüh,<sup>1,4,6,\*</sup> and Helmut Kettenmann<sup>1,5,6,7,\*</sup>

<sup>1</sup>Cellular Neuroscience, Max-Delbrück-Center for Molecular Medicine in the Helmholtz Association, Robert Roessle Strasse 10, 13125 Berlin, Germany

<sup>2</sup>Charité-Universitätsmedizin, 10117 Berlin, Germany

<sup>3</sup>Department of Neurosurgery, Tongji Hospital of Tongji Medical College of Huazhong University of Science and Technology, 430030 Wuhan, China

<sup>4</sup>Department of Neurosurgery, University Medical Center Schleswig-Holstein, 24105 Kiel, Germany

<sup>5</sup>Shenzhen Institute of Advanced Technology, Chinese Academy of Sciences, Shenzhen, China

<sup>6</sup>These authors contributed equally

<sup>7</sup>Lead contact

\*Correspondence: [charlotte.flueh@uksh.de](mailto:charlotte.flueh@uksh.de) (C.F.), [kettenmann@mdc-berlin.de](mailto:kettenmann@mdc-berlin.de) (H.K.)

<https://doi.org/10.1016/j.celrep.2022.110670>

## SUMMARY

Factors released from glioma-associated microglia/macrophages (GAMs) play a crucial role in glioblastoma multiforme (GBM) progression. Here, we study the importance of CCL18, a cytokine expressed in human but not in rodent GAMs, as a modulator of glioma growth. Since CCL18 signaling could not be studied in classical mouse glioma models, we developed an approach by transplanting induced pluripotent stem cell-derived human microglia and human glioma cells into mouse brain slices depleted of their intrinsic microglia. We observe that CCL18 promotes glioma cell growth and invasion. Chemokine (C-C motif) receptor 8 (CCR8) is identified as a functional receptor for CCL18 on glioma cells, and ACP5 (acid phosphatase 5) is revealed as an important part of the downstream signaling cascade for mediating glioma growth. We conclude, based on the results from an *in vitro*, *ex vivo* humanized glioma model and an *in vivo* GBM model that microglia/macrophage-derived CCL18 promotes glioma growth.

## INTRODUCTION

Glioma is the most common primary malignant tumor in the brain. Current strategies including surgical resection followed by radiotherapy, chemotherapy, and newly introduced tumor-treating fields prolong survival time of patients with GBM, but the overall median survival time of patients with GBM is still merely 12–16 months (Anthony et al., 2018; Gutmann and Kettenmann, 2019). The glioma microenvironment has attracted increasing attention in the past decade since it became evident that it creates an immune-suppressive and pro-tumorigenic environment (Sampson et al., 2020). Glioma-associated microglia/macrophages (GAMs), which make up 30%–50% of the tumor mass, now have been established as a crucial element modulating glioma cell growth or chemotherapy/radiotherapy resistance (Gutmann and Kettenmann, 2019). Multiple pathways have been identified as crucial signaling pathways between GAMs and glioma, which resulted in novel approaches for clinical trials (Gutmann and Kettenmann, 2019).

CCL18 belongs to the CC chemokine family and is mainly produced by myeloid cells (Schutyser, 2005). Recently, CCL18 was found to play a pivotal role in the development of several types

of peripheral cancers (Liu et al., 2019; Meng et al., 2015; Zhao et al., 2020), while its role in glioma remains largely unknown. While CCL18 is expressed in human cells, it lacks murine ortholog (Schutyser, 2005), and as a result, its action cannot be analyzed in the classical murine experimental glioma models. Recently protocols have been established to generate human microglia from induced pluripotent stem cells (iPSC) (McQuade et al., 2018). These human stem cell-derived microglial cells (iMGL) have been implanted into mice generating chimeric models where the properties of iMGL can be studied in a tissue environment (Svoboda et al., 2019). In this study we generated the humanized GAMs-glioma *ex vivo* model using human iMGL and human glioma cells (cell line- and patient-derived primary GBM cells) to systematically investigate the source and role of CCL18 in the glioma context.

## RESULTS

### A humanized tissue model to study CCL18-mediated microglia-glioma interaction

In order to investigate the role of CCL18, which is expressed in humans, but not in rodents, we developed a model to study the interaction of human glioma cells with human microglia in a



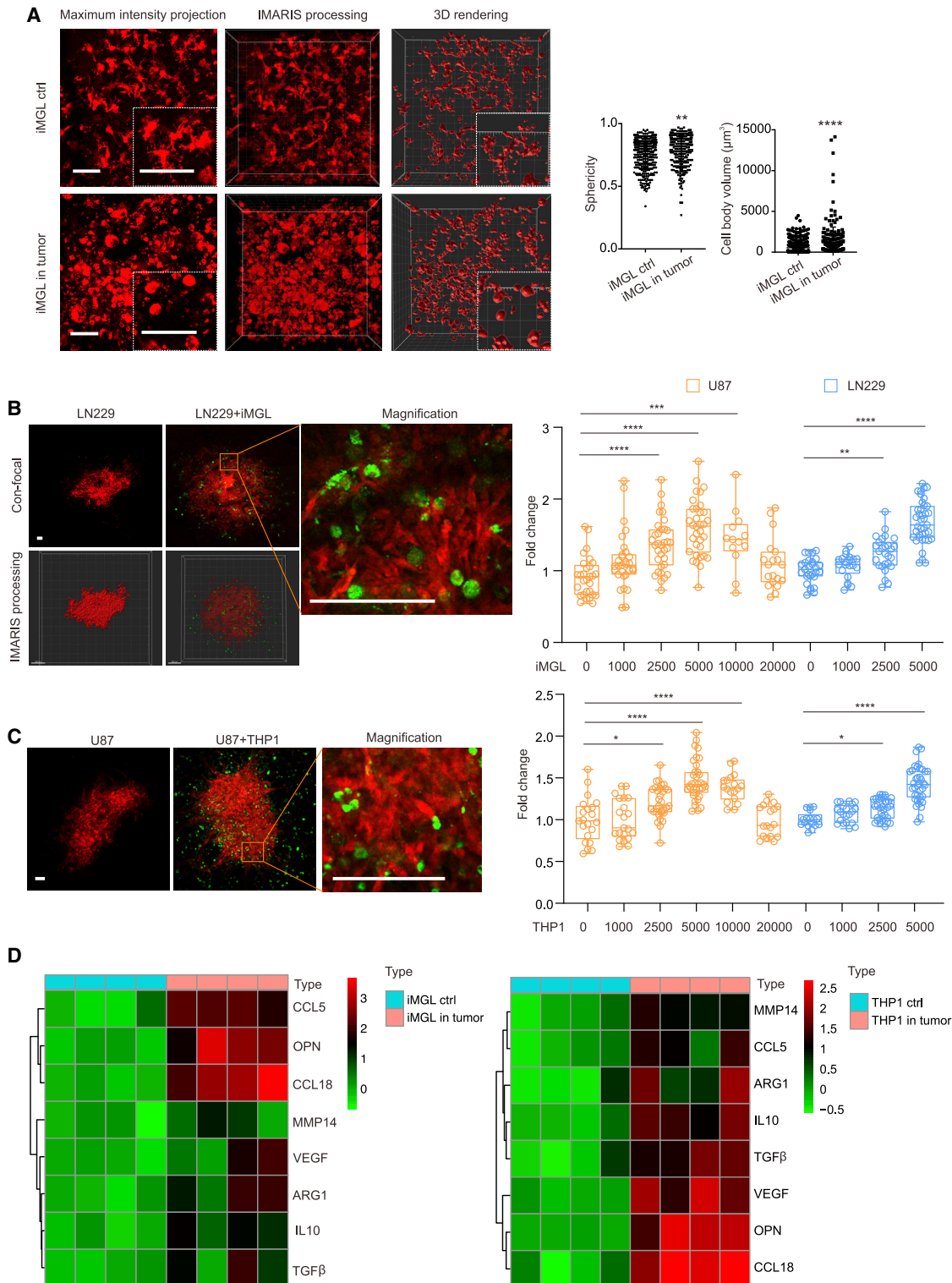


**Figure 1. A humanized tissue model to study microglia-glioma interaction**

(A) iMGL were injected with or without glioma into murine microglia-depleted organotypic brain slices (OBSs). Morphology of iMGL stained with Iba-1 in the murine OBSs are shown as maximum intensity projection and after 3D rendering using IMARIS software. The upper images are from slices injected with iMGL only, and the lower images are from slices co-injected with glioma and iMGL within the tumor area. The insets present the enlarged images of iMGL morphology.

(legend continued on next page)

tissue context. We depleted intrinsic microglia from murine organotypic brain slices (OBSs) and injected either human glioma cells alone or in combination with the human iMGL. The differentiation procedure and characterization of iMGL from Xmo01-hiPSC is shown in Figure S1. In addition, the efficiency of endogenous microglia depletion is also presented in Figure S1. We determined sphericity and cell body volume of iMGL with or without presence of tumor cells by iba-1 staining followed by 3D rendering using IMARIS software. iMGL co-injected with glioma cells (LN229-mCherry) showed a higher level of sphericity and cell body volume, indicating that the tumor microenvironment affected the morphology of iMGL (Figure 1A). Subsequently we determined the tumor volume. The presence of microglia significantly increased the glioma volume generated by U87MG and LN229 with different ratios of glioma cell and microglia. In addition, tumor volume of the glioma cell lines U87MG, U251MG, LN229, and patient-derived glioma cells co-injected with microglia at a ratio of 2:1 (glioma cell:microglia) was also assessed in Figure S2. Co-injecting the human monocyte cell line THP-1 also resulted in a larger glioma volume (Figure 1C).

iMGL or macrophages were isolated from the OBSs 5 days after injection together with LN229-mCherry and were sorted by magnetic activated cell sorting (MACS) using CD11b-beads. We compared glioma-associated iMGL that were co-injected with LN229-mCherry cells with iMGL injected alone. The expression level of genes that are known to be upregulated by the glioma environment was compared in glioma associated and naive iMGL. Interleukin 10 (IL10), Osteopontin (OPN), matrix metallo proteinase 14 (MMP14), vascular endothelial growth factor (VEGF), transforming growth factor  $\beta$  (TGF  $\beta$ ), and CCL18 were significantly upregulated (Figure 1D). Similar results were obtained for THP-1-derived macrophage cells, except for the upregulation of MMP14 (Figure 1D). Taken together, our humanized model showed that iMGL and THP-1 cells resulted in larger tumors and upregulation of similar genes as in glioma-associated murine microglia.

### Bioinformatic analysis revealed that CCL18 was expressed the highest in the human GAMs and negatively correlated to survival time with GBM

We compared our previously published RNA-seq dataset of normal human microglia and GAMs (Szulzewsky et al., 2016)

with the murine GAMs RNA-seq dataset (Szulzewsky et al., 2015) and identified 319 genes that are only upregulated in human GAMs but not in murine (Figure 2A, left). Among these 319 genes, we found 11 genes that were expressed in human brains but not in mouse brains (Bitar et al., 2019), thus being human specific (Figure 2A, right). Moreover, we evaluated the correlation between the expression of these 11 human-specific genes with the level of macrophage infiltration based on Tumor Immune Estimation Resource (TIMER, <http://timer.comp-genomics.org/>) (Li et al., 2016, 2020) using the human TCGA GBM RNA-seq database and found that only CCL18 and amphiregulin (AREG) positively correlated to the GAMs infiltration level (using Rho value of Spearman's test), with CCL18 showing the best correlation (Figures 2B and S3).

We therefore performed a systematic meta-analysis on TCGA GBM RNA-seq/HU133A and TCGA Agilent 4502A as well as TCGA GBMLGG RNA-seq database utilizing the bioinformatics platform GLIOVIS (<http://gliovis.bioinfo.cnio.es/>) (Bowman et al., 2017). CCL18 mRNA was expressed much higher in GBM tissue compared to normal brain tissue (Figures 2C–2E). Also, based on the data from TCGA GBMLGG RNA-seq database, CCL18 mRNA expression was higher in GBM when compared to other type of gliomas and also higher in WHO grade IV gliomas compared to lower grades (Figures S4A and S4B).

We also analyzed the correlation between CCL18 expression and medium survival of patients with GBM in three different GBM databases. In all databases, there was a positive correlation between higher CCL18 expression and lower median survival (CGGA GBM database, Figure S4C; TCGA GBM RNA-seq, Figure S4D; TCGA GBM HG-U133A, Figure S4E), indicating that CCL18 correlated with a worse outcome for the patients. Besides, a detailed subset of IDH WT/MUT analysis (in TCGA GBM RNA-seq) showed that CCL18 gene expression negatively correlated with survival time of patients with IDHWT GBM (Figure S4F). Furthermore, primary and recurrent GBM were also assessed in the TCGA GBM RNA-seq, which indicated that higher CCL18 expression level was correlated with shorter survival time in both patients with primary and recurrent GBM (Figure S4F).

### CCL18 is mainly expressed by GAMs in glioma

To verify that CCL18 was expressed in GBM tissue and GAMs, we stained fresh slices from human GBM and human cortex

Sphericity and cell body volume of iMGL were quantified and are shown on the right. Bar, 50  $\mu$ m. (n = 5 per group, unpaired Student's t test, \*\* = p < 0.01, \*\*\*\* = p < 0.0001).

(B) 5,000 red fluorescence-labeled LN229-mCherry glioma cells were inoculated alone (left image) or together with 5,000 DiD-labeled (green) iMGL (right image) into murine microglia-depleted OBSs. The area shown on the middle upper image is shown in a magnified image on the right. Bar = 100  $\mu$ m. The quantification of the tumor volumes for 5,000 U87MG-mCherry and 5,000 LN229-mCherry glioma cell line co-injected with different numbers of iMGL (from 1,000 to 20,000) were assessed. The graph on the right shows the relative fold change of tumor volumes normalized to controls (0). (n = 6 per group, at least two tumors per n, one-way ANOVA with Tukey's post hoc test, \*\* = p < 0.01, \*\*\* = p < 0.001, \*\*\*\* = p < 0.0001).

(C) Similar to the experiment described in (B), 5,000 DiD-labeled human THP-1-derived macrophages (green) and 5,000 U87MG-mCherry (red) were injected into murine microglia-depleted OBSs. The image on the right is a magnification of the area shown in the middle image. Bar, 100  $\mu$ m. The quantification of the tumor volumes for 5,000 U87MG-mCherry and 5,000 LN229-mCherry glioma cell line co-injected with different numbers of THP-1 macrophages (from 1,000 to 20,000) were evaluated. The graph on the right shows the relative fold change of tumor volumes normalized to controls (0). (n = 6 per group, at least two tumors per n, one-way ANOVA with Tukey's post hoc test, \* = p < 0.05, \*\*\*\* = p < 0.0001).

(D) Expression of a set of genes in slices inoculated with 5,000 iMGL or 5,000 iMGL and 5,000 LN229 glioma cells (on the left) or 5,000 THP-1 or 5,000 THP-1 and 5,000 LN229 glioma cells (on the right). The slices were maintained for 5 days, and subsequently the tissue was dissociated. qPCR was performed to compare expression level of CD11b<sup>+</sup> cells in the slices with (in tumor) or without glioma cells (ctrl). The heatmap shows the Log<sub>2</sub> fold change (Log<sub>2</sub>FC) of the listed genes (n = 4 per group).

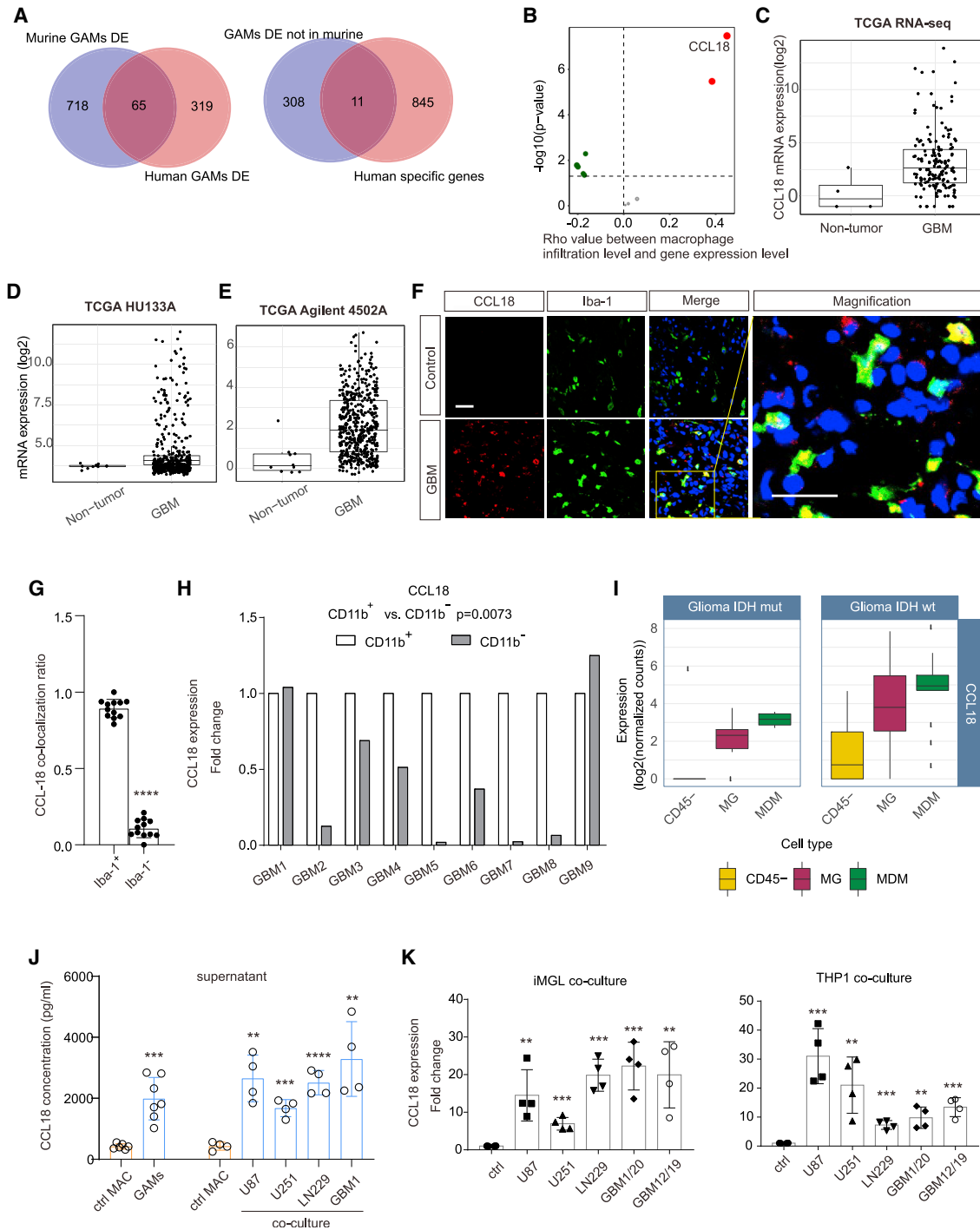


**Figure 2. CCL18 is highly expressed in the human GAMs**

(A) On the left, Venn's diagram shows the overlap of upregulated genes in murine GAMs compared to control microglia in the RNA-seq database (murine GAMs differentially expressed genes [DE]) and human GAMs RNA-seq dataset (Human GAM DE) with 319 genes only upregulated in human GAMs. On the right, Venn's diagram illustrates the comparison between the genes only upregulated in human GAMs (GAMs DE not in murine) and human-specific genes (not expressed in rodents) in brain tissue identifying 11 genes.

(B) The Rho value of correlation between macrophage infiltration level (based on TIMER algorithm) and gene expression of the 11 human-specific genes (using TCGA RNA-seq expression value) identified in (A).

(C) Gene expression of CCL18 in human GBM and normal brain tissue obtained from the TCGA GBM RNA-seq database.

(D) Gene expression of CCL18 comparing human GBM and normal brain tissue obtained from the TCGA GBM HU-133A database.

(legend continued on next page)

from a patient with acute trauma as a non-tumorous control, for CCL18 and the GAM specific marker Iba-1. As shown in Figure 2F, CCL18 expression was higher in the GBM specimen compared with the trauma tissue. Moreover, CCL18 is predominantly co-localized with Iba-1 (Figures 2F and 2G). We also separated GAMs from other cells of human GBM tissue by MACS sorting using CD11b beads. The CD11b<sup>+</sup> cells displayed a significantly higher level of CCL18 expression than the CD11b<sup>-</sup> population from a cohort of nine patients (Figure 2H). To further confirm that CCL18 expression was higher in GAMs compared with other cells in glioma, we used the TCGA RNA-seq database and analyzed the correlation between the expression level of CCL18 and GAM-specific genes (Iba-1, CD68, CD11b). Indeed, there was a positive correlation between the expression level of GAM-specific genes and CCL18 (Figure S4G). Besides, based on TCGA GBM RNA-seq dataset, we found a strong positive correlation between GAM infiltration and CCL18 mRNA expression using Cell types enrichment analysis (xCell, <https://xcell.ucsf.edu>) on TIMER platform (Figure S4H). To further validate that CCL18 is primarily expressed by GAMs in GBM, we analyzed the Brain Tumor Immune Micro Environment dataset (<https://joycelab.shinyapps.io/braintime/>) (Klemm et al., 2020), and we found that CCL18 expression was significantly higher in microglia or macrophages compared to CD45<sup>-</sup> cells (Figure 2I). Furthermore, we compared the CCL18 protein level in the supernatant of blood monocyte-derived macrophages (ctrl MAC) from healthy donors with MACS sorted GAMs from patient-derived GBM, and we observed a significantly increased level of CCL18 in the supernatant (Figure 2J). To study whether the glioma environment leads to a release of CCL18, we cocultured blood monocyte-derived macrophages (ctrl MAC) from healthy donors with human glioma cell lines (U87MG, U251MG, LN229) or patient-derived primary glioma cells (GBM1) for 72 h, and after medium change for 24 h, the supernatant was collected and the CCL18 protein level was determined by ELISA. A significantly higher level of CCL18 was found in the supernatant when macrophages were cocultured with glioma cells (Figure 2J). Moreover, iMGL was cocultured with human glioma cell lines U87, U251, LN229, and patient-derived primary glioma cells (GBM1/20, GBM12/19) for 72 h, and CCL18 mRNA expression on iMGL was determined by real-time quantitative PCR (qPCR). As shown in Figure 2K (left), CCL18 was upregulated in all cocultures. A similar upregulation of CCL18 was

also found for the human macrophage cell line THP-1 (Figure 2K, right). Taken together, our data illustrate that CCL18 is predominantly expressed and released by GAMs in the glioma environment.

### CCL18 released from GAMs influences glioma growth

To study the effect of CCL18 on glioma growth, we took advantage of our humanized *ex vivo* model described earlier, injected murine slices with U87MG, U251MG, and LN229 glioma cells and glioma cells isolated from a patient together with iMGL and used a CCL18 neutralizing antibody (aCCL18) to affect CCL18 levels, which resulted in a smaller tumor volume (Figure 3A). Similar results were obtained when OBSs were injected with THP-1 cells and glioma cells (Figure 3B).

To demonstrate that CCL18 was released from microglia, we compared the effect of the neutralizing antibody on glioma growth after injection of glioma cells without microglia or macrophages (U251MG, LN229, and patient-derived cells). The neutralizing antibody was not effective in reducing glioma growth when microglial cells or macrophages were absent (Figure S5).

We also tested whether CCL18 affected glioma proliferation and expansion. The glioma cell lines U87MG, U251MG, and LN229 and two patient-derived primary glioma cells were treated with different concentrations (1, 10, 100 ng/mL) of human recombinant CCL18 (rCCL18), and the proliferating activities were determined by CCK-8 kit. This treatment significantly increased glioma cell proliferation in all glioma cell lines at 100 ng/mL, in three at 10 ng/mL (U87MG, LN229, and one patient line), and in LN229 cells even at 1 ng/mL (Figure 3C). A colony formation assay was used to study glioma expansion. Here we found that a higher number of colonies appeared in the CCL18-treated LN229 cells and two patient-derived glioma cell lines (Figure 3D). Furthermore, Ki-67 staining of the glioma cell lines U87MG, U251MG, and LN229 and two patient-derived primary glioma cells revealed that 100 ng/mL CCL18 treatment significantly increased the percentage of Ki-67<sup>+</sup> cells (Figure 3E). Taken together, these data illustrate that CCL18 promotes glioma cell growth.

Next, we examined the effect of CCL18 on glioma cell migration via a wound healing assay and Boyden chamber assay. CCL18 enhanced the migratory activity of LN229, U87MG, and U251MG glioma cells at 100 ng/mL and in U87MG and U251MG even at 10 ng/mL in the wound healing assay

(E) Gene expression of CCL18 comparing human GBM and normal brain tissue obtained from the TCGA GBM Agilent-4502A database.

(F) Immunofluorescence staining of patient-derived GBM slices and non-malignant brain cortex tissue (control) from patients with traumatic brain injury. Bar, 100  $\mu$ m.

(G) Co-localization of CCL18 expression with Iba-1-positive (+) and Iba-1-negative cells (-) in GBM specimen given as ratio.

(H) CCL18 gene expression of CD11b-positive (CD11b<sup>+</sup>) and CD11b-negative (CD11b<sup>-</sup>) cells separated from nine patient-derived GBMs by MACs (paired Student's t test).

(I) CCL18 gene expression of the CD45-negative cell population (CD45<sup>-</sup>), microglia (MG), and macrophages (MDM) in human glioma with IDH mutations ( $\mu$ ) and IDH wild-type (wt) using Brain Tumor Immune Micro Environment dataset.

(J) CCL18 concentration was determined in the supernatant by ELISA in blood monocyte-derived macrophages (ctrl MAC) from healthy donors ( $n = 6$ ) and in MACS sorted GAMs from patient-derived GBM ( $n = 7$ ) (left two bars, unpaired Student's t test, \*\*\* =  $p < 0.001$ ). The right five columns show the CCL18 concentration in the supernatant from control macrophages (ctrl MAC) and from macrophages cocultured with the glioma lines U87, U251, LN229, and patient-derived primary glioma cells (GBM1) ( $n = 4$  per group, one-way ANOVA with Tukey's post hoc test, \*\* =  $p < 0.01$ , \*\*\* =  $p < 0.001$ , \*\*\*\* =  $p < 0.0001$ ).

(K) CCL18 gene expression determined by qPCR in iMGL (left) and THP-1 cells (right) cocultured with the glioma cell lines U87MG, U251MG, LN229, and two patient-derived cell lines (GBM1/20, GBM12/19). The data are normalized to iMGL or THP-1 cultured without glioma cells (ctrl). ( $n = 4$  per group, one-way ANOVA with Tukey's post hoc test, \*\* =  $p < 0.01$ , \*\*\* =  $p < 0.001$ ).

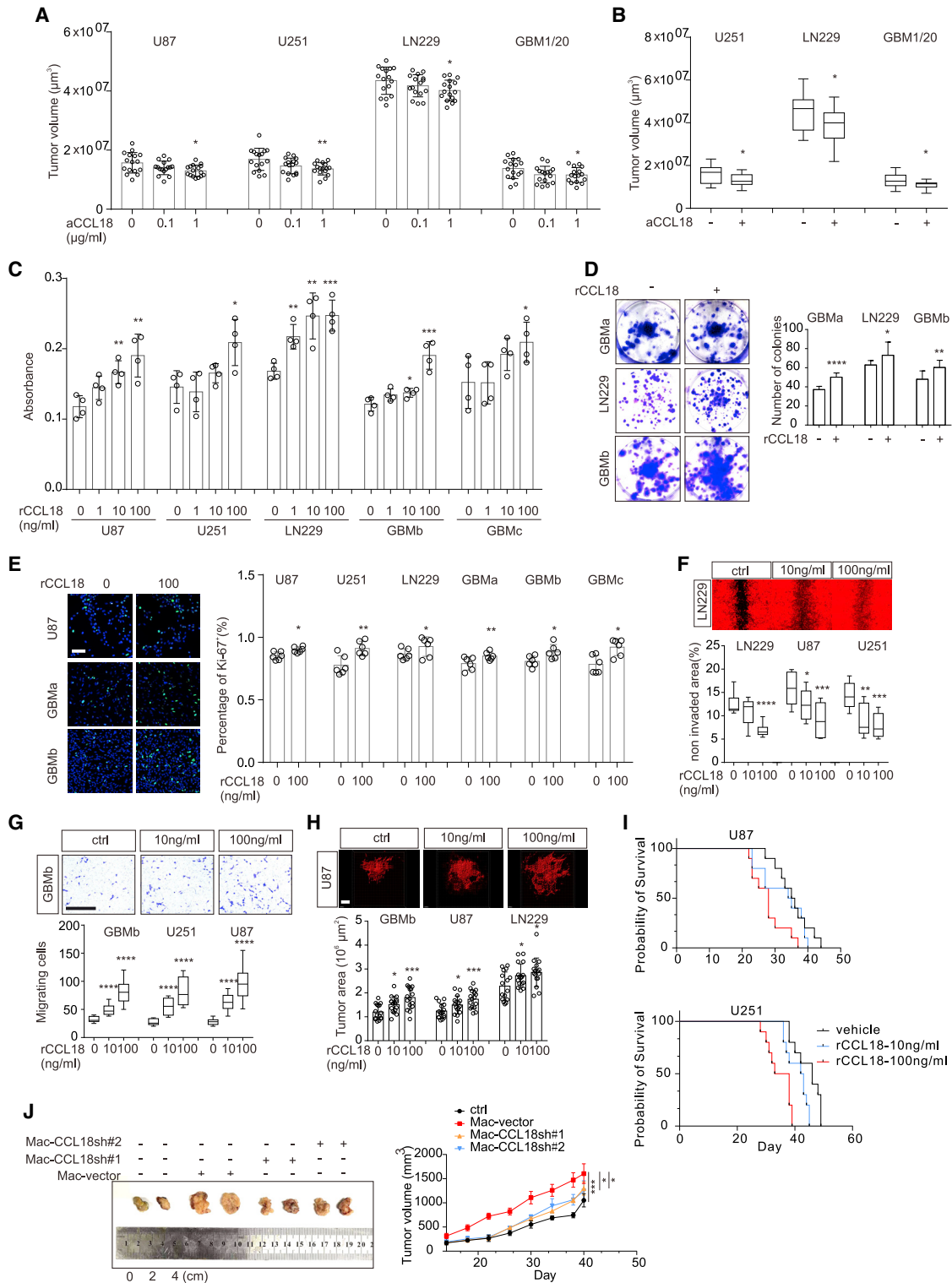


**Figure 3. CCL18 promotes glioma cell proliferation, migration, and invasion**

(A) Fluorescence-labeled glioma cells (U87MG-mCherry, U251MG-mCherry, and LN229-mCherry) and DiD-labeled patient-derived glioma cells (GBM1/20) were inoculated together with DiD-labeled iMGL into OBSs. Slices were treated with 1  $\mu\text{g/ml}$  isotype (0), 0.1 or 1  $\mu\text{g/ml}$  CCL18 neutralizing antibody (aCCL18), and tumor volumes were quantified. (n = 6 per group, at least two tumors per n, one-way ANOVA with Tukey's post hoc test, \* = p < 0.05, \*\* = p < 0.01).

(legend continued on next page)

(Figure 3F). In the Boyden chamber assay, cell migration of U251MG and U87MG and a patient-derived glioma cell line was enhanced at 10 and 100 ng/mL of CCL18 (Figure 3G). To investigate the role of CCL18 on glioma cell invasion, murine OBSs were generated and intrinsic microglia were depleted to remove the influence of murine microglia. mCherry fluorescence-labeled glioma cells (U87MG-mCherry and LN229-mCherry) and DiD fluorescence-labeled patient-derived primary glioma cells (GBM1/20) were inoculated into the OBSs and were treated with CCL18. We found that treatment with 10 ng/mL and 100 ng/mL CCL18 resulted in significantly larger tumor areas (Figure 3H). To further verify the tumor-promoting effect of CCL18 *in vivo*, U87MG or U251MG glioma cells were inoculated into the brains of nude mice, and recombinant CCL18 was injected into the tumor at day 7 and day 14 after tumor inoculation. We observed a significantly shorter survival time of tumor mice injected with CCL18 (Figure 3I). Furthermore, THP-1-derived macrophages together with U251MG glioma cells (1:1) were subcutaneously injected into nude mice and tumor volume were assessed. Here we also observed significant larger tumors when U251MG were co-injected with THP-1 macrophages, while the tumor-promoting effect was attenuated when CCL18 was knocked down by two different CCL18 shRNA in THP-1 macrophages (Figure 3J). The corresponding knockdown efficiency was determined by qPCR (Figure S7A). In conclusion, CCL18 enhances the migration and invasion of glioma cells.

### CCR8 expressed on tumor cell acts as functional receptor for CCL18

CCR8 is a receptor for CCL18 and is expressed by different types of tumor cells (Liu et al., 2019; Tsuboi et al., 2020). We could

confirm that CCR8 expression was high in GBM tissue based on the TCGA GBM databases (Figures S6A–S6C) and was negatively correlated to patient survival (Figure S6D). Furthermore, higher CCR8 mRNA expression correlated with a shorter survival time in patients with IDH WT GBM as well as primary GBM (Figure S6E). We then assessed the CCR8 expression in the GBM slices from patients and found that CCR8 was highly expressed in glioma cells (Iba-1 negative cells) compared with non-malignant human brain tissue (Figure 4A). We separated CD11b<sup>+</sup> and CD11b<sup>−</sup> cells from patient-derived glioma tissue and found that CCR8 was predominantly expressed by CD11b<sup>−</sup> cells (Figure 4B). To test whether CCR8 acted as a functional receptor for CCL18 in glioma cells, we stimulated proliferation of glioma cells with CCL18 and applied a CCR8 neutralizing antibody. The CCL18-induced increase of proliferating activity as determined by the CCK-8 kit was largely attenuated by the CCR8 neutralizing antibody (Figure 4C). For a further functional test, we measured tumor growth in (murine microglia-depleted) OBSs inoculated with U251MG, LN229, and patient-derived glioma cells. The CCR8 neutralizing antibody abolished the CCL18-induced increase in tumor growth (Figure 4D). Using the siRNA and shRNA approach, we knocked down CCR8 expression in U251MG and LN229 glioma cells. These knockdowns efficiently silenced CCR8 expression and lasted for 5 days, as determined by qPCR and immunofluorescence staining (Figures S7B–S7D). We then inoculated the CCR8 knockdown glioma cells (U251MG and LN229) into OBSs. CCL18 treatment did not increase tumor growth, while this was observed in control glioma cells (Figure 4E). Furthermore, iMGL were co-inoculated with glioma cells into OBSs and tumor growth was monitored. Although the co-injection with iMGL increased tumor growth in control glioma cells, this effect was abolished in the

- (B) Fluorescence-labeled glioma cells (U251MG-mCherry, LN229-mCherry) and DiD-labeled patient-derived glioma cells (GBM1/20) were inoculated together with DiD-labeled THP-1-derived macrophages into OBSs. Slices were treated with 1 μg/mL isotype control or 1 μg/mL CCL18 neutralizing antibody (aCCL18), and tumor volumes were quantified. (n = 6 per group, at least two tumors per n, unpaired Student's t test, \* = p < 0.05).
- (C) Glioma cells (U87MG, U251MG, LN229) and two patient-derived cells (GBMb, GBMc) were treated with 1, 10, or 100 ng/mL recombinant CCL18 (rCCL18) for 48 h compared to vehicle control (0). Proliferation activity of the cells was measured as absorbance using the CCK-8 kit. (n = 4 per group, one-way ANOVA with Tukey's post hoc test, \* = p < 0.05, \*\* = p < 0.01, \*\*\* = p < 0.001).
- (D) Patient-derived glioma cells (GBMa) and the U87MG cells were treated with 100 ng/mL recombinant CCL18 (rCCL18) for 14 days, and the colonies of the cells were labeled by crystal violet staining. Quantification of the colonies is shown in the graph on the left. (n = 4 per group, unpaired Student's t test, \* = p < 0.05, \*\* = p < 0.01, \*\*\*\* = p < 0.0001).
- (E) Patient-derived glioma cells (GBMa, GBMb) and the U87MG cells were treated with 100 ng/mL recombinant CCL18 (rCCL18) for 48 h compared to vehicle treated cells (0). Proliferating activity of the cells was assessed by immunofluorescence staining of Ki-67 (green) and DAPI (blue). Bar, 100 μm. Representative images are shown on the left, and quantification of Ki-67<sup>+</sup> cells is shown on the right. (n = 6 per group, unpaired Student's t test, \* = p < 0.05, \*\* = p < 0.01).
- (F) Fluorescence-labeled glioma cells (U87MG-mCherry, U251MG-mCherry, and LN229-mCherry) were scratch wounded and treated with 10 and 100 ng/mL recombinant CCL18 (rCCL18) for 24 h. Representative figures are shown on top, and the quantification of the migratory activity into the cell-free zone is shown below as the percentage of the cell-free zone after 24 h compared to the beginning of the experiment. (n = 4 per group, one-way ANOVA with Tukey's post hoc test, \* = p < 0.05, \*\* = p < 0.01, \*\*\*\* = p < 0.0001).
- (G) Boyden chamber assay was used to determine chemotaxis of patient-derived glioma cells (GBMb), U87MG and U251MG cells in a gradient of 10 or 100 ng/mL recombinant CCL18 (rCCL18) compared to vehicle control (ctrl). Bar, 200 μm. Representative figures of stained cells are shown on top, and quantification of the migrating cells is shown below. (n = 4 per group, one-way ANOVA with Tukey's post hoc test, \*\*\*\* = p < 0.0001).
- (H) Fluorescence-labeled glioma cells (U87MG-mCherry, LN229-mCherry) and DiD-labeled primary glioma cells (GBMb) were inoculated into murine microglia-depleted OBSs and treated with 10 or 100 ng/mL recombinant CCL18 (rCCL18) compared to vehicle control (ctrl). Bar, 300 μm. Representative images of the 3D rendered tumor area are shown on top, with the quantification below. (n = 6 per group, at least two tumors per n, one-way ANOVA with Tukey's post hoc test, \* = p < 0.05, \*\*\* = p < 0.001).
- (I) U87MG (upper graph) or U251MG (lower graph) glioma cells were inoculated into brains of nude mice and 10 ng or 100 ng of recombinant CCL18 (rCCL18) were intratumorally injected on day 7 and day 14 after tumor inoculation compared to vehicle injection. Survival time of the mice was recorded. (n = 10 per group). Log rank (Mantel-Cox) test was used to compare the difference of survival time.
- (J) U251MG glioma cells were co-injected with negative control vector transfected THP-1 macrophages (MAC vector-co) or CCL18 shRNA transfected THP-1 macrophages (MAC CCL18sh#1 or MAC CCL18sh#2). Tumor volumes were monitored every 3–40 days post tumor injection. Representative figures of the tumors are shown on the left, with the quantification on the right. (n = 6 per group, one-way ANOVA with Tukey's post hoc test, \* = p < 0.05, \*\*\* = p < 0.001).

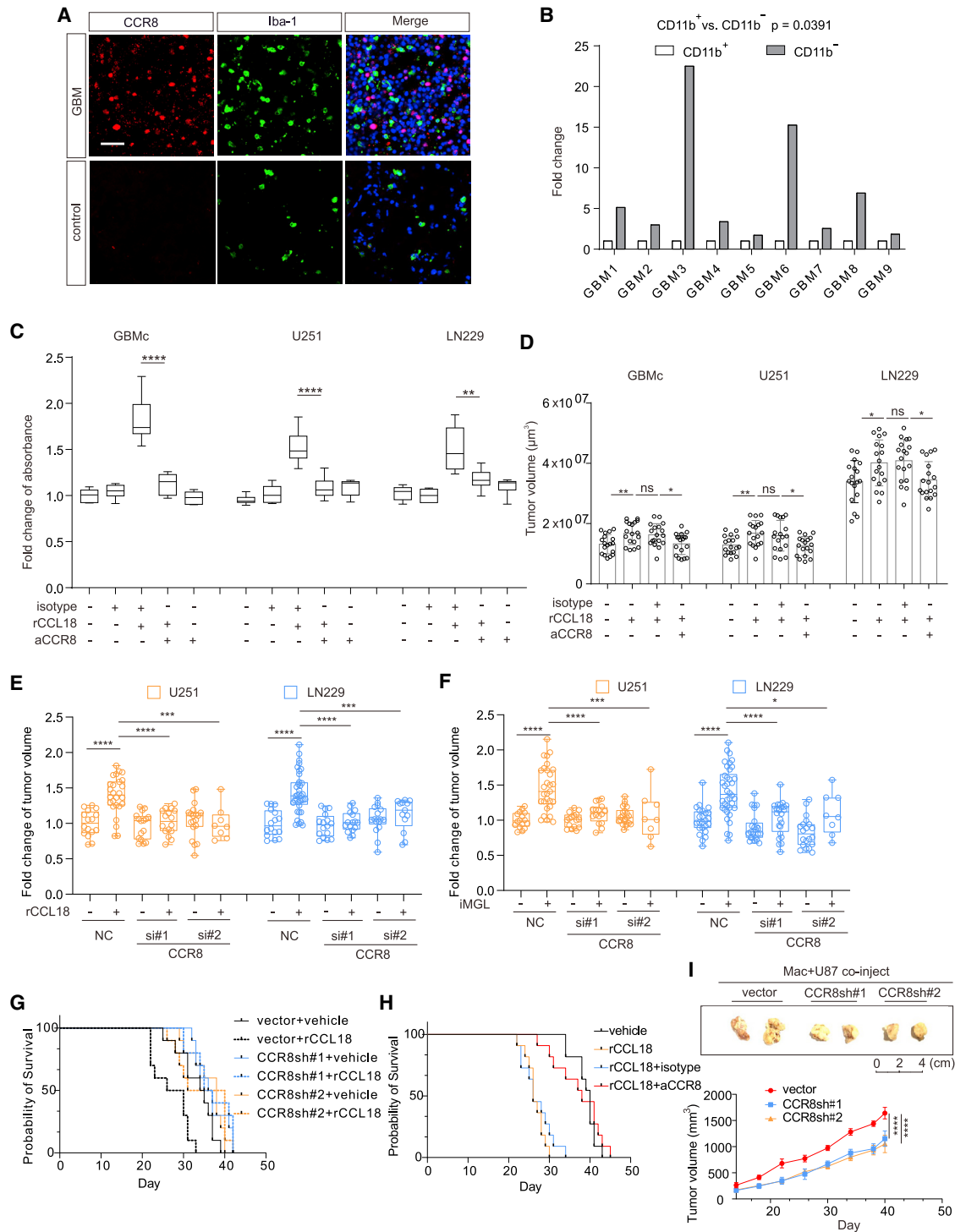


**Figure 4. CCR8 on tumor cells acts as functional receptor for CCL18**

(A) Immunofluorescence staining of patient-derived GBM slices and brain cortex tissue from patients with traumatic brain injury (control) with CCR8 (red, left), Iba-1 (green, middle), and merged with DAPI (blue, right). Bar denotes 100 μm.

(B) CCR8 gene expression was compared between CD11b-positive (CD11b<sup>+</sup>) and CD11b-negative (CD11b<sup>-</sup>) cells separated from nine patient-derived GBM tissues by MACs as fold change relative to the CD11b-positive cells (paired Student's t test).

(legend continued on next page)

CCR8 knockdown glioma cells (Figure 4F). To further verify this effect *in vivo*, we knocked down CCR8 in U251MG cells, inoculated these cells into the brains of nude mice, and treated the tumor with CCL18. In the CCR8-deficient tumors, CCL18 treatment had no effect on the survival time (Figure 4G), while CCR8 knockdown alone did not alter glioma growth (Figure 4G). In addition, we blocked CCR8 by adding a CCR8 neutralizing antibody and found that CCR8 blockade successfully attenuated the CCL18 effect (Figure 4H). Moreover, tumor volumes were also assessed *in vivo* by subcutaneously injecting CCR8 knockdown glioma cells (U251MG) with THP-1 macrophages. The tumors generated by the glioma cells with CCR8 knockdown were significantly smaller (Figure 4I). Since G protein-coupled receptor 30 (GPR30) and membrane-associated phosphatidylinositol transfer protein 3 (PITPNM3) have also been identified as CCL18 receptors in other tissues, we performed a meta-analysis on TCGA GBM RNA-seq and found that GPR30 expression was at a similar level in GBM and normal brain based on the GEPIA database (<http://gepia2.cancer-pku.cn/>) (Tang et al., 2019) (Figure S8A), while expression of PITPNM3 was even lower in GBM using GLIOVIS database (Figure S8B). Moreover, to validate this on the protein level, we stained the GBM specimens for GPR30 and PITPNM3. Only PITPNM3 was detectable in GBM specimens (Figure S8C). To test the importance of PITPNM3 for CCL18 signaling, we knocked down PITPNM3 by siRNA in U251MG glioma cells. Unlike the knockdown of CCR8, PITPNM3 silencing did not affect the tumor-promoting effect of CCL18 (Figure S8D), suggesting that PITPNM3 was not important for CCL18 signaling in gliomas. In summary, CCR8 is expressed by glioma cells and mediates CCL18 signaling and its functional effects on glioma growth.

### CCL18-induced glioma cell growth is regulated by downstream protein ACP5

Since CCL18 promoted glioma cell growth via CCR8 receptor, we checked for pathways of downstream signaling. We

performed a meta-analysis correlating CCL18 expression with the genes in the TCGA GBM HGU133A database. We found 1,476 genes that were significantly correlated with CCL18 expression using Pearson's product-moment correlation analysis. Acid phosphatase 5 (ACP5) showed the highest correlation (Figure 5A). Looking into the TCGA GBM RNA-seq (Figure 5B, left) and TCGA GBM HGU133A (Figure 5B, right) databases confirmed the strong correlation between CCL18 and ACP5 expression ( $r = 0.7741$ , left of Figure 5B;  $r = 0.781$ , right of Figure 5B). ACP5, also called tartrate-resistant acid phosphatase, is a glycosylated monomeric metalloprotein enzyme. It has been reported that ACP5 promotes tumor metastasis in multiple solid cancers (Bian et al., 2019; Xia et al., 2014), although it has not been studied in glioma. ACP5 was highly expressed in human GBM compared to normal brain in TCGA GBM RNA-seq datasets (Figure 5C). Also, ACP5 protein expression was found in patient GBM slices (Figure 5D), while co-localization of GAM-specific markers (Iba-1) and ACP5 in the tissue was low, indicating that ACP5 was mainly expressed by tumor cells.

To experimentally examine the relationship between CCL18 and ACP5, we treated glioma cells with CCL18 and determined ACP5 gene expression by qPCR. Treatment with CCL18 induced a significant upregulation of ACP5 in U251MG, LN229, and patient-derived glioma cells (Figure 5E). This upregulation was validated by immunofluorescence staining of ACP5 in LN229 glioma cells (Figure 5F), suggesting that CCL18 upregulates downstream ACP5 expression in glioma cells. Besides, CCR8 knockdown notably abolished the CCL18-mediated ACP5 upregulation, indicating that ACP5 is located downstream of CCL18/CCR8 activation (Figure 5F).

To determine the role of ACP5 in the CCL18-induced tumor promotion, we silenced the ACP5 gene in glioma cells (U251MG and LN229) via ACP5 siRNA and treated them with CCL18. We found that the CCL18-induced proliferation was attenuated when ACP5 was knocked down as assessed by

(C) Proliferating activity of patient-derived cells (GBMc), U251MG and LN229 cells treated with recombinant CCL18 (rCCL18, 100 ng/mL), CCR8 neutralizing antibody (aCCR8, 0.5  $\mu$ g/mL), and isotype control antibody (isotype, 0.5  $\mu$ g/mL) was quantified by the CCK-8 kit. The absorbance is shown in relation to the untreated control. (n = 6 per group, \*\* =  $p < 0.01$ , \*\*\*\* =  $p < 0.0001$ ).

(D) Patient-derived cells (GBMc) and U251MG-mCherry and LN229-mCherry glioma cells were inoculated into OBSs and were treated with recombinant CCL18 (rCCL18, 100 ng/mL), CCR8 neutralizing antibody (aCCR8, 0.5  $\mu$ g/mL), and isotype control antibody (isotype, 0.5  $\mu$ g/mL). Tumor volumes are illustrated in the graph. (n = 6 per group, at least two tumors per n, one-way ANOVA with Tukey's post hoc test, \* =  $p < 0.05$ , \*\* =  $p < 0.01$ , ns = no significance).

(E) Two different CCR8 siRNA were used to silence CCR8 in U251MG-mCherry and LN229-mCherry glioma cells. Negative control (NC) or CCR8 siRNA (si#1 and si#2) transfected U251MG-mCherry and LN229-mCherry glioma cells were inoculated into OBSs and treated with recombinant CCL18 (rCCL18, 100 ng/mL). Tumor volumes were quantified, and relative fold change of tumor volumes is presented. (n = 7 per group, at least two tumors per n, one-way ANOVA with Tukey's post hoc test, \*\*\* =  $p < 0.001$ , \*\*\*\* =  $p < 0.0001$ ).

(F) Negative control (NC) or CCR8 siRNA (si#1 and si#2) transfected U251MG-mCherry or LN229-mCherry glioma cells were co-inoculated with IMGL into OBSs. Tumor volumes were quantified, and relative fold change of tumor volumes is presented. (n = 7 per group, at least two tumors per n, one-way ANOVA with Tukey's post hoc test, \* =  $p < 0.05$ , \*\*\* =  $p < 0.001$ , \*\*\*\* =  $p < 0.0001$ ).

(G) Two different CCR8 shRNA were used to knock down CCR8 in U251MG glioma cells. Negative control (vector) or CCR8 shRNA (CCR8sh#1 and CCR8sh#2) transfected U251MG glioma cells were inoculated into brains of nude mice. Vehicle solution (vehicle) or recombinant CCL18 (rCCL18, 10 or 100 ng) was intratumorally injected on day 7 and day 14 after tumor injection. The survival curve shown here represents the survival time of tumor-bearing mice. (n = 10 per group). Log rank (Mantel-Cox) test was used to compare the difference of survival time.

(H) U251MG glioma cells were inoculated into brains of nude mice. Vehicle solution (vehicle) or recombinant CCL18 (rCCL18, 100 ng) was injected into the tumor on day 7 and day 14 after the initial tumor injection. For CCR8 inhibition, CCR8 neutralizing antibody (aCCR8, 1  $\mu$ g) or isotype IgG (isotype, 1  $\mu$ g) was intraperitoneally injected into tumor-bearing mice every other day. Survival curve represent the survival time of tumor-bearing mice. (n = 11 per group). Log rank (Mantel-Cox) test was used to compare the difference of survival time.

(I) Negative control (vector) or CCR8 shRNA (CCR8sh#1 and CCR8sh#2) transfected U87MG glioma cells were subcutaneously co-injected with THP-1 macrophages (Mac) into nude mice. Tumor volumes were monitored every 3–40 days post tumor injection. Representative tumor volumes are presented on top and the summarized data below. (n = 6 per group, one-way ANOVA with Tukey's post hoc test, \*\*\*\* =  $p < 0.0001$ ).

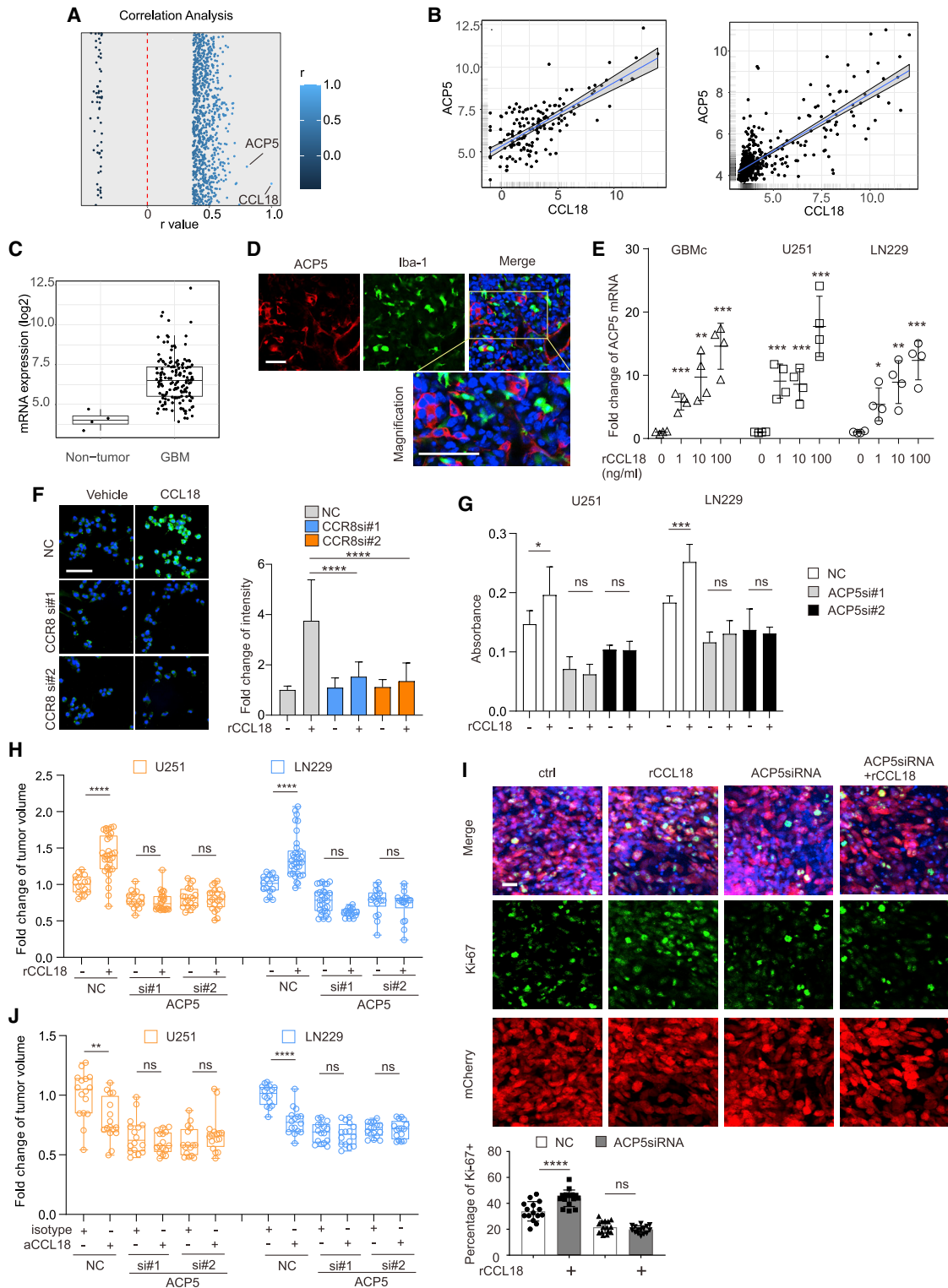


**Figure 5. CCL18-induced glioma cell growth is regulated by ACP5**

(A) Correlation analysis of genes that are significantly correlated to CCL18 in the TCGA GBM U133A database. Each spot represents one gene. ACP5 showed the highest correlation as indicated.

(B) Correlation between CCL18 and ACP5 expression in the TCGA GBM RNA-seq (left) and TCGA GBM U133A (right) database.

(C) Comparison of ACP5 expression level between normal brain tissue and GBM in TCGA GBM RNA-seq database.

(legend continued on next page)

CCK-8 kit (Figure 5G). Furthermore, we validated the results by inoculating ACP5 siRNA-silenced glioma cells into OBSs. The CCL18-induced tumor growth as determined in control cells was not observed in the siRNA-silenced glioma cells (Figure 5H). Moreover, these slices were stained with proliferation indicator Ki-67. Here, we observed that ACP5 silencing on tumor cells abolished the CCL18-induced increase in Ki-67-positive cells (Figure 5I).

To test whether the reduction of glioma growth induced by the antibody against CCL18 depends on ACP5 expression, U251MG and LN229 control or ACP5-silenced glioma cells were co-injected with iMGL into OBSs. The glioma growth-inhibiting effect of the antibody was observed in the control cells, but not in the siRNA-silenced glioma cells (Figure 5J). Since we observed a lower proliferation rate of glioma cells when silencing ACP5, glioma cells with ACP5 silencing were also treated with IL-1beta and C-C motif ligand 5 (CCL5), which has previously been shown to promote tumor growth (Gutmann and Kettenmann, 2019; Lu et al., 2020; Xue et al., 2019; Gutmann and Kettenmann, 2019; Yu-Ju Wu et al., 2020). ACP5 silencing did not alter the tumor-promoting effect of either IL-1beta or CCL5 (Figures S9A and S9B).

### CCL18 promotes glioma cell growth via Akt/PRAS40 signaling cascade

To unravel the signaling cascade activated by CCL18 in glioma cells, Proteome Profiler Human Phospho-Kinase Array was used to screen the potential signaling targets on CCL18-treated LN229 cells. Phosphorylated-proline-rich protein (p-PRAS40) was expressed significantly higher in the CCL18-treated glioma cells (Figure 6A). PRAS40 is a substrate of Akt signaling and serves to transduce Akt signals to the mTOR complex. Also, it was described previously that PRAS40 regulated tumor cell growth and metastasis (Lv et al., 2017). Therefore, we confirmed the upregulation of p-PRAS40 in glioma cells after CCL18 stimulation (Figure 6B). Moreover, since Akt signals upstream of PRAS40, we confirmed that CCL18 increased the active form

of Akt (phosphorylated Akt) expression level in the glioma cells (Figure 6B). To again verify that CCR8 acts as a functional receptor of CCL18, CCR8 knockdown glioma cells were stimulated with CCL18. CCL18 stimulation failed to activate either PRAS40 or Akt (Figure 6C). To clarify whether ACP5 was the initiator of the Akt/PRAS40 signaling, ACP5 knockdown glioma cells were stimulated with CCL18. CCL18 stimulation failed to stimulate Akt and p-PRAS40 (Figure 6D), indicating that Akt/PRAS40 signaling is regulated by ACP5. Furthermore, glioma cells were treated with the Akt inhibitors Wortmannin and LY294002, followed by CCL18 treatment. Indeed, Akt signaling inhibition abolished CCL18-induced glioma growth (Figure 6E). Taken together, we demonstrate that CCL18 promotes glioma growth via the Akt/PRAS40 signaling pathway.

### DISCUSSION

In this study, we focused on a signaling pathway for the communication between GAMs and glioma cells, which are expressed in humans but not in rodents, and we established a humanized *ex vivo* brain slice model to study the interaction between human glioma cells and GAMs. Using bioinformatic analysis on our previously published GAMs sequencing dataset on human and murine cells, we identified 319 genes that were upregulated in human but not in murine tissue. Among these genes, 11 were expressed by humans and not by mice. One of the most prominently expressed genes was CCL18, and its expression level was linked to a worse clinical outcome. We found that in a glioma context, GAMs were the main source of CCL18, while its expression was low in glioma cells. In the non-malignant brain tissue, its expression also was low, and it was upregulated in microglia and macrophages in a glioma context.

In glioma, microglia/macrophages are polarized to a defined phenotype that leads to glioma progression (Gutmann and Kettenmann, 2019). Multiple interactions between GAMs and glioma have been reported, such as the Versican-TLR2-MMP14 signaling pathway or miRNA-TLR7 axis, indicating complex

(D) Immunofluorescence staining of patient-derived GBM slices with ACP5 (red, left), Iba-1 (green, middle), and merged with DAPI (blue, right). The image below is a magnified view of the merged image. Bar, 50  $\mu$ m.

(E) Patient-derived glioma cells (GBM<sub>c</sub>) and the glioma lines U251MG and LN229 treated with 1, 10, or 100 ng/mL recombinant CCL18 (rCCL18) for 6 h, and ACP5 gene expression was detected by qPCR. Expression is normalized to unstimulated control (0). (n = 4 per group, one-way ANOVA with Tukey's post hoc test, \* =  $p < 0.05$ , \*\* =  $p < 0.01$ , \*\*\* =  $p < 0.001$ ).

(F) Negative control (NC) or CCR8 siRNA (CCR8 si#1 and CCR8 si#2) transfected LN229 glioma cells were treated with 100 ng/mL recombinant CCL18 (rCCL18) for 48 h, and ACP5 protein expression was detected by immunofluorescence (ACP5, green; DAPI, blue). Scale bar, 50  $\mu$ m. The fluorescence intensity is quantified in the graph on the right. (n = 4 per group, one-way ANOVA with Tukey's post hoc test, \*\*\*\* =  $p < 0.0001$ ).

(G) Proliferation activity detected as absorbance by CCK-8 kit of U251MG and LN229 cells pre-transfected with two ACP5 siRNA (gray bars, ACP5si#1; black bars, ACP5si#2) or negative control (white bars, NC) and additionally treated with recombinant CCL18 (rCCL18, 100 ng/mL) for 48 h. The absorbance is given in arbitrary units. (n = 6 per group, one-way ANOVA with Tukey's post hoc test, \* =  $p < 0.05$ , \*\*\* =  $p < 0.001$ , ns = no significance).

(H) Negative control (NC) or ACP5 siRNA (ACP5 si#1 and ACP5 si#2) transfected U251MG-mCherry (left) and LN229-mCherry glioma cells (right) were injected into OBSs. Subsequently slices were treated with recombinant CCL18 (rCCL18, 100 ng/mL) for 5 days. Tumor volumes were quantified, and relative fold change of tumor volumes is presented. (n = 7 per group, at least two tumors per n, one-way ANOVA with Tukey's post hoc test, \*\*\*\* =  $p < 0.0001$ , ns = no significance).

(I) Slices generated in (H) injected with LN229 cells either non-transfected (two left images) or transfected with ACP5 siRNA (si#1, two right images) and treated with recombinant CCL18 as indicated were stained with Ki-67 (green, middle images) and combined images of Ki-67; mCherry with DAPI (blue) is shown on top (merge). The tumor cells are labeled by the mCherry fluorescence (lower images). Quantification of Ki-67-positive cells in the tumor area is shown below. Bar, 50  $\mu$ m. (n = 7 per group, at least two tumors per n, one-way ANOVA with Tukey's post hoc test, \*\*\*\* =  $p < 0.0001$ , ns = no significance).

(J) Tumor volumes of U251MG (left) and LN229 glioma cells (right) co-inoculated with iMGL into OBSs and pre-treated with ACP5 siRNA (gray bars) compared to an untreated control (white bars, NC). Subsequently slices were treated with antibody against CCL18 (aCCL18, 1  $\mu$ g/mL) or an isotype control antibody (isotype, 1  $\mu$ g/mL) for 5 days. Tumor volumes were quantified, and relative fold change of tumor volumes is presented. (n = 7 per group, at least two tumors per n, one-way ANOVA with Tukey's post hoc test, \*\* =  $p < 0.01$ , \*\*\*\* =  $p < 0.0001$ , ns = no significance).

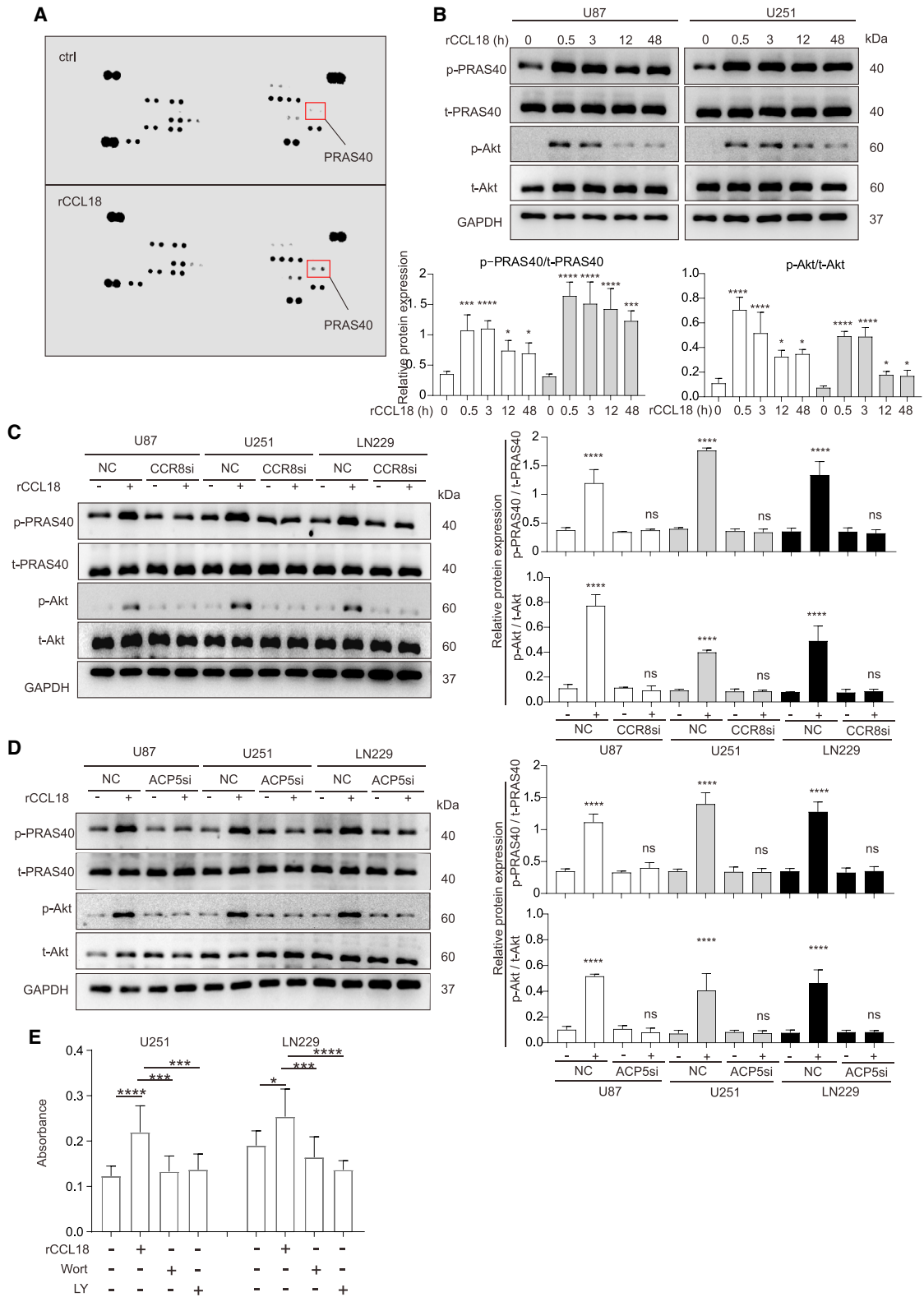


**Figure 6. CCL18 promotes glioma cell growth via Akt/PRAS40**

(A) Proteome Profiler Human Phospho-Kinase Array shows the different phospho-kinase of LN229 glioma cells after CCL18 treatment (rCCL18, 100 ng/mL) compared to vehicle control (ctrl). Note the increase in p-PRAS40.

(legend continued on next page)

mechanisms in how GAMs impact tumor cells (Buonfiglioli et al., 2019; Vinnakota et al., 2013). All these previous studies used mouse models to analyze the functional interaction between GAMs and glioma cells and to characterize these pathways on a molecular level in a tissue context. To analyze the functional interactions between GAMs and glioma cells mediated by CCL18 signaling, we developed an approach, namely the humanized mouse brain slice. Recently it became possible to generate microglial cells from iPSCs (Hirbec et al., 2020; McQuade et al., 2018). These cells can be implanted into a mouse brain where they acquire microglial features (Hasselmann et al., 2019). We have now established a protocol where we implanted human iMGL and/or human glioma cells into cultured murine brain slices, which were depleted of their intrinsic microglia before. This model allowed us to manipulate these human cells in a tissue context, which is not possible *in vivo*. We could verify data from the murine system, showing that human microglia promote human glioma growth. We also found that genes that were upregulated in mouse microglia are also upregulated in human iMGL when confronted with glioma cells. To show the importance of CCL18 for microglia/glioma interaction, we could demonstrate that a CCL18 neutralizing antibody attenuated the microglia-enhanced glioma growth. This effect required the presence of microglia.

To date, there are three receptors that have been proposed for CCL18: PTPN13, GPR30, and CCR8. It has been demonstrated that PTPN13 is expressed in several types of solid cancer, for instance breast cancer cells (Chen et al., 2011), and GPR30 is expressed in lung cancer (Schmidt-Wolf and Zissel, 2020). In glioma, both bioinformatics analysis as well as our staining of glioma tissue revealed that GPR30 expression was very low in GBM. Our experiments illustrated that PTPN13 does not mediate CCL18 signaling in the glioma context. Therefore, we were able to demonstrate that CCR8 is expressed in glioma cells and serves as functional receptor for CCL18 similarly as reported for other cell types (Brix et al., 2015; Liu et al., 2019). Using our humanized mouse model, we could further demonstrate that the expression of CCR8 is essential for the CCL18-mediated effect on glioma growth.

Employing a bioinformatic analysis to search for CCL18/CCR8-triggered intracellular pathways, we identified ACP5, a metalloenzyme, which mediates tumor cell proliferation and migration potentially through extracellular matrix digestion and

epithelial-mesenchymal transition (Bian et al., 2019). Indeed, we observed that ACP5 knockdown in glioma cells largely attenuated their growth and expansion mediated by CCL18. Furthermore we found that the Akt/PRAS40 signaling pathway is activated by ACP5, and this signaling cascade could serve as a further target for interfering with CCL18/CCR8 signaling.

CCL18, as a type of chemokine, has chemotactic functions for the innate immune system (Schutyser, 2005). CCL18 was also reported to have protumorigenic effect in several types of solid cancers. We found that CCL18 promotes both glioma cell growth and protumorigenic effect migration.

We have not yet addressed the mechanism by which glioma cells induce the upregulation of CCL18 in microglial cells. It has been demonstrated for monocytes that Toll-like receptor-2 regulates CCL18 expression. We previously found that TLR2 upregulates microglial MMP14 expression, which promotes glioma cell expansion (Vinnakota et al., 2013). Thus, taken together, we speculate that glioma cells modulate GAMs to upregulate CCL18, which in turn activates CCR8 receptor on the glioma cells. Via ACP5 signaling it promotes glioma growth and invasion. Thus interfering with the CCL18-CCR8-ACP5 pathway may be a potential target for glioma suppression.

#### Limitations of the study

Our study established a humanized glioma model to study interaction between human glioma and GAMs using iPSC-derived human microglia. However, this model does not determine the influence of other microenvironment components such as T lymphocytes, dendritic cells, or endothelial cells, which may also participate in CCL18 signaling. Besides, orthotopic *in vivo* experiments using human iMGL to generate glioma were not presented in this study.

#### STAR★METHODS

Detailed methods are provided in the online version of this paper and include the following:

- KEY RESOURCES TABLE
- RESOURCE AVAILABILITY
  - Lead contact
  - Materials availability
  - Data and code availability

(B) Western blot shows the phosphorylated PRAS40 (p-PRAS40), total PRAS40 (t-PRAS40), phosphorylated Akt (p-Akt), total Akt (t-Akt), and GAPDH expression in glioma lines U87MG and U251MG treated with 100 ng/mL CCL18 for 0.5, 3, 12, and 48 h, respectively, compared to vehicle control (0). Quantification of the blot is presented below as relative expression of p-PRAS40 normalized to t-PRAS40 and p-Akt normalized to t-Akt. (n = 4 per group, one-way ANOVA with Tukey's post hoc test, \* = p < 0.05, \*\*\* = p < 0.001, \*\*\*\* = p < 0.0001).

(C) Negative control (NC) and CCR8 siRNA (CCR8si) transfected cells of U87MG, U251MG, as well as LN229 cell lines were treated with 100 ng/mL recombinant CCL18 (rCCL18) for 30 min. Western blot shows the phosphorylated PRAS40 (p-PRAS40), total PRAS40 (t-PRAS40), phosphorylated Akt (p-Akt), total Akt (t-Akt), and GAPDH expression. Quantification of the blot is presented on the right as relative expression of p-PRAS40 normalized to t-PRAS40 and p-Akt normalized to t-Akt. (n = 4 per group, one-way ANOVA with Tukey's post hoc test, \*\*\*\* = p < 0.0001, ns = no significance).

(D) Negative control (NC) and ACP5 siRNA (ACP5si) transfected glioma cell lines U87MG, U251MG, as well as LN229 were treated with 100 ng/mL recombinant CCL18 (rCCL18) for 30 min. The western blot shows the phosphorylated PRAS40 (p-PRAS40), total PRAS40 (t-PRAS40), phosphorylated Akt (p-Akt), and total Akt (t-Akt). Quantification of the blot is presented on the right as relative expression of p-PRAS40 normalized to t-PRAS40 and p-Akt normalized to t-Akt. (n = 4 per group, one-way ANOVA with Tukey's post hoc test, \*\*\*\* = p < 0.0001, ns = no significance).

(E) Glioma cell lines U251MG and LN229 treated with 5 μM Wortmannin (Wort) and 5 μM LY294002 (LY) together with 100 ng/mL recombinant CCL18 (rCCL18) for 48 h. Cell proliferation was assessed as absorbance by CCK-8 kit. (n = 6 per group, one-way ANOVA with Tukey's post hoc test, \* = p < 0.05, \*\*\* = p < 0.001, \*\*\*\* = p < 0.0001).

● EXPERIMENTAL MODEL AND SUBJECT DETAILS

- Animals
- Human material
- Cell culture

● METHOD DETAILS

- Bioinformatic analysis of TCGA GBM data and GEO dataset
- *In vitro* differentiation of iMGL
- Human GAM isolation by magnetic activated cell sorting (MACS)
- Small interfering RNA (siRNA) and short hairpin RNA (shRNA) mediated genes knockdown
- Organotypic brain slice (OBS) model and tumor inoculation
- CCK-8 counting kit and scratch (wound healing) assay
- Transwell assay and colony formation assay
- Glioma xenografts
- Immunofluorescent staining
- Real-time quantitative PCR (qPCR)
- Enzyme linked immunosorbent assay (ELISA)
- Western blot
- Proteome profiler™ human phospho-kinase array

● QUANTIFICATION AND STATISTICAL ANALYSIS

SUPPLEMENTAL INFORMATION

Supplemental information can be found online at <https://doi.org/10.1016/j.celrep.2022.110670>.

ACKNOWLEDGMENTS

We thank Regina Piske, Maren Wendt, Nadine Scharek, and Michaela Seeger-Zografakis for technical assistance, the microscopy core facility (Advanced Light Microscopy, ALM) and the stem core cell facility of the MDC Berlin for technical assistance. We also thank China Scholarship Council (CSC) for funding a stipend for Y.H. This work was supported by Einstein-Stiftung, the Helmholtz-Gemeinschaft, Zukunftsthema "Immunology and Inflammation" (ZT-0027), and the Berlin Institute of Health (BIH).

AUTHOR CONTRIBUTIONS

H.K. and C.F. conceptualized and supervised the study. H.K., C.F., and Y.H. wrote the manuscript with input from all other authors. Y.H., E.M., C.N., L.K., Y.Y., P.X., M.L., S.Z., M.S., N.Q., H.Z., T.L., and F.H. carried out the experiments and analyzed and/or discussed data. Specifically, Y.H., E.M., C.N., Y.Y., P.X., M.L., S.Z., and N.Q. performed the OBS model and other experiments (including qPCR, western blot, immunohistochemistry, measuring cell proliferation and migration). L.K. and M.S. performed the differentiation of iPSC cells. H.Z., T.L., and F.H. helped with analyzing and/or discussion of the data. C.F. and M.S. collected the human biopsies.

DECLARATION OF INTERESTS

The authors declare no competing interests.

Received: March 12, 2021  
Revised: February 21, 2022  
Accepted: March 21, 2022  
Published: April 12, 2022

REFERENCES

- Anthony, P., McArdle, S., and McHugh, M. (2018). Tumor treating fields: adjuvant treatment for high-grade gliomas. *Semin. Oncol. Nurs.* **34**, 454–464.
- Bian, Z.-Q., Luo, Y., Guo, F., Huang, Y.-Z., Zhong, M., and Cao, H. (2019). Overexpressed ACP5 has prognostic value in colorectal cancer and promotes cell proliferation and tumorigenesis via FAK/PI3K/AKT signaling pathway. *Am. J. Cancer Res.* **9**, 22–35.
- Bitar, M., Kuiper, S., O'Brien, E.A., and Barry, G. (2019). Genes with human-specific features are primarily involved with brain, immune and metabolic evolution. *BMC Bioinform.* **20**, 406.
- Bowman, R.L., Wang, Q., Carro, A., Verhaak, R.G.W., and Squatrito, M. (2017). Gliovis data portal for visualization and analysis of brain tumor expression datasets. *Neuro. Oncol.* **19**, 139–141.
- Brix, S.R., Stege, G., Disteldorf, E., Hoxha, E., Krebs, C., Krohn, S., Otto, B., Klätschke, K., Herden, E., Heymann, F., et al. (2015). CC chemokine ligand 18 in ANCA-associated crescentic GN. *J. Am. Soc. Nephrol.* **26**, 2105–2117.
- Buonfiglioli, A., Efe, I.E., Guneykaya, D., Ivanov, A., Huang, Y., Orlowski, E., Krüger, C., Deisz, R.A., Markovic, D., Flüh, C., et al. (2019). Iet-7 MicroRNAs regulate microglial function and suppress glioma growth through toll-like receptor 7. *Cell Rep.* **29**, 3460–3471.e7.
- Chen, J., Yao, Y., Gong, C., Yu, F., Su, S., Chen, J., Liu, B., Deng, H., Wang, F., Lin, L., et al. (2011). CCL18 from tumor-associated macrophages promotes breast cancer metastasis via PTPN23. *Cancer Cell* **19**, 541–555.
- Gutmann, D.H., and Kettenmann, H. (2019). Microglia/brain macrophages as central drivers of brain tumor pathobiology. *Neuron* **104**, 442–449.
- Hasselmann, J., Coburn, M.A., England, W., Figueroa Velez, D.X., Kiani Shabestari, S., Tu, C.H., McQuade, A., Kolahehdouzan, M., Echeverria, K., Claes, C., et al. (2019). Development of a chimeric model to study and manipulate human microglia in vivo. *Neuron* **103**, 1016–1033.e10.
- Hirbec, H., Déglon, N., Foo, L.C., Goshen, I., Grutzendler, J., Hangen, E., Kreisler, T., Linck, N., Muffat, J., Regio, S., et al. (2020). Emerging technologies to study glial cells. *Glia* **68**, 1692–1728.
- Hu, F., Dzaye, O.D.A., Hahn, A., Yu, Y., Scavetta, R.J., Dittmar, G., Kaczmarek, A.K., Dunning, K.R., Ricciardelli, C., Rinnenthal, J.L., et al. (2015). Glioma-derived versican promotes tumor expansion via glioma-associated microglial/macrophages Toll-like receptor 2 signaling. *Neuro. Oncol.* **17**, 200–210.
- Huang, Y., Zhang, Q., Lubas, M., Yuan, Y., Yalcin, F., Efe, I.E., Xia, P., Motta, E., Buonfiglioli, A., Lehnardt, S., et al. (2020). Synergistic toll-like receptor 3/9 signaling affects properties and impairs glioma-promoting activity of microglia. *J. Neurosci.* **40**, 6428–6443.
- Klemm, F., Maas, R.R., Bowman, R.L., Kornete, M., Soukup, K., Nassiri, S., Brouland, J.P., Iacobuzio-Donahue, C.A., Brennan, C., Tabar, V., et al. (2020). Interrogation of the microenvironmental landscape in brain tumors reveals disease-specific alterations of immune cells. *Cell* **181**, 1643–1660.e17.
- Li, B., Severson, E., Pignon, J.C., Zhao, H., Li, T., Novak, J., Jiang, P., Shen, H., Aster, J.C., Rodig, S., et al. (2016). Comprehensive analyses of tumor immunity: implications for cancer immunotherapy. *Genome Biol.* **17**, 174.
- Li, T., Fu, J., Zeng, Z., Cohen, D., Li, J., Chen, Q., Li, B., and Liu, X.S. (2020). TIMER2.0 for analysis of tumor-infiltrating immune cells. *Nucleic Acids Res.* **48**, W509–W514.
- Liu, X., Xu, X., Deng, W., Huang, M., Wu, Y., Zhou, Z., Zhu, K., Wang, Y., Cheng, X., Zhou, X., et al. (2019). CCL18 enhances migration, invasion and EMT by binding CCR8 in bladder cancer cells. *Mol. Med. Rep.* **19**, 1678–1686.
- Lu, J., Xu, Z., Duan, H., Ji, H., Zhen, Z., Li, B., Wang, H., Tang, H., Zhou, J., Guo, T., et al. (2020). Tumor-associated macrophage interleukin-β promotes glycerol-3-phosphate dehydrogenase activation, glycolysis and tumorigenesis in glioma cells. *Cancer Sci.* **111**, 1979–1990.
- Lv, D., Guo, L., Zhang, T., and Huang, L. (2017). PRAS40 signaling in tumor. *Oncotarget* **8**, 69076–69085.
- Markovic, D.S., Vinnakota, K., Chirasani, S., Synowitz, M., Raguet, H., Stock, K., Sliwa, M., Lehmann, S., Kälin, R., Van Rooijen, N., et al. (2009). Gliomas

induce and exploit microglial MT1-MMP expression for tumor expansion. *Proc. Natl. Acad. Sci. U S A*. *106*, 12530–12535.

McQuade, A., Coburn, M., Tu, C.H., Hasselmann, J., Davtyan, H., and Blurton-Jones, M. (2018). Development and validation of a simplified method to generate human microglia from pluripotent stem cells. *Mol. Neurodegener.* *13*, 67.

Meng, F., Li, W., Li, C., Gao, Z., Guo, K., and Song, S. (2015). CCL18 promotes epithelial-mesenchymal transition, invasion and migration of pancreatic cancer cells in pancreatic ductal adenocarcinoma. *Int. J. Oncol.* *46*, 1109–1120.

Neftel, C., Laffy, J., Filbin, M.G., Hara, T., Shore, M.E., Rahme, G.J., Richman, A.R., Silverbush, D., Shaw, M.L., Hebert, C.M., et al. (2019). An integrative model of cellular States, plasticity, and genetics for glioblastoma. *Cell* *178*, 835–849.e21.

Sampson, J.H., Gunn, M.D., Fecci, P.E., and Ashley, D.M. (2020). Brain immunology and immunotherapy in brain tumours. *Nat. Rev. Cancer* *20*, 12–25.

Sasmono, R.T., and Williams, E. (2012). Generation and characterization of MacGreen mice, the Cfs1r-EGFP transgenic mice. *Methods Mol. Biol.* *844*, 157–176.

Schmidt-Wolf, R., and Zissel, G. (2020). Interaction between CCL18 and GPR30 differs from the interaction between estradiol and GPR30. *Anticancer Res.* *40*, 3097–3108.

Schutysse, E. (2005). Involvement of CC chemokine ligand 18 (CCL18) in normal and pathological processes. *J. Leukoc. Biol.* *78*, 14–26.

Svoboda, D.S., Barrasa, M.I., Shu, J., Rietjens, R., Zhang, S., Mitalipova, M., Berube, P., Fu, D., Shultz, L.D., Bell, G.W., et al. (2019). Human iPSC-derived microglia assume a primary microglia-like state after transplantation into the neonatal mouse brain. *Proc. Natl. Acad. Sci. U S A*. *116*, 25293–25303.

Szulzewsky, F., Pelz, A., Feng, X., Synowitz, M., Markovic, D., Langmann, T., Holtman, I.R., Wang, X., Eggen, B.J.L., Boddeke, H.W.G.M., et al. (2015). Glioma-associated microglia/macrophages display an expression profile

different from M1 and M2 polarization and highly express Gpnmb and Spp1. *PLoS One* *10*, e0116644.

Szulzewsky, F., Arora, S., de Witte, L., Ulas, T., Markovic, D., Schultze, J.L., Holland, E.C., Synowitz, M., Wolf, S.A., and Kettenmann, H. (2016). Human glioblastoma-associated microglia/monocytes express a distinct RNA profile compared to human control and murine samples. *Glia* *64*, 1416–1436.

Tang, Z., Kang, B., Li, C., Chen, T., and Zhang, Z. (2019). GEPIA2: an enhanced web server for large-scale expression profiling and interactive analysis. *Nucleic Acids Res.* *47*, W556–W560.

Tsuboi, H., Iizuka-Koga, M., Asashima, H., Takahashi, H., Kudo, H., Ono, Y., Honda, F., Iizuka, A., Segawa, S., Abe, S., et al. (2020). Upregulation and pathogenic roles of CCL18-CCR8 axis in IgG4-related disease. *Mod. Rheumatol.* *30*, 729–737.

Vinnakota, K., Hu, F., Ku, M.C., Georgieva, P.B., Szulzewsky, F., Pohlmann, A., Waiczies, S., Waiczies, H., Niendorf, T., Lehnardt, S., et al. (2013). Toll-like receptor 2 mediates microglia/brain macrophage MT1-MMP expression and glioma expansion. *Neuro. Oncol.* *15*, 1457–1468.

Xia, L., Huang, W., Tian, D., Chen, Z., Zhang, L., Li, Y., Hu, H., Liu, J., Chen, Z., Tang, G., et al. (2014). ACP5, a direct transcriptional target of FoxM1, promotes tumor metastasis and indicates poor prognosis in hepatocellular carcinoma. *Oncogene* *33*, 1395–1406.

Xue, L., Lu, B., Gao, B., Shi, Y., Xu, J., Yang, R., Xu, B., and Ding, P. (2019). NLRP3 promotes glioma cell proliferation and invasion via the interleukin-1b/NF- $\kappa$ B p65 signals. *Oncol. Res.* *27*, 557–564.

Yu-Ju Wu, C., Chen, C.H., Lin, C.Y., Feng, L.Y., Lin, Y.C., Wei, K.C., Huang, C.Y., Fang, J.Y., and Chen, P.Y. (2020). CCL5 of glioma-associated microglia/macrophages regulates glioma migration and invasion via calcium-dependent matrix metalloproteinase 2. *Neuro. Oncol.*

Zhao, C., Zheng, S., Yan, Z., Deng, Z., Wang, R., and Zhang, B. (2020). CCL18 promotes the invasion and metastasis of breast cancer through Annexin A2. *Oncol. Rep.* *43*, 571–580.

## STAR★METHODS

### KEY RESOURCES TABLE

REAGENT or RESOURCE	SOURCE	IDENTIFIER
<b>Antibodies</b>		
Goat Anti-Iba-1 polyclonal antibody	Abcam	Cat#ab5076, RRID:AB_2224402
Rabbit Anti-TMEM119 antibody	Invitrogen	Cat#PA5-62661, RRID: AB_2648508
Rabbit anti-P2Y12 antibody	Genetex	Cat# GTX54796
Rabbit anti-CCL18 antibody	Invitrogen	Cat# PA5-46817, RRID:AB_2608478
Rabbit anti-CCL18 antibody	Invitrogen	Cat# PA5-46817, RRID:AB_2608478
Rabbit Anti-Ki-67 antibody	Abcam	Cat#ab15580, RRID:AB_443209
Rabbit anti-CCR8 antibody	Invitrogen	Cat#PA5-34633, RRID: AB_2551985
Rabbit anti-GPR30 antibody	Abcam	Cat#ab39742, RRID: AB_1141090
Rabbit anti-PITPNM3 antibody	Invitrogen	Cat#PA5-54589, RRID:AB_2645583
Mouse anti-ACP5 antibody	Invitrogen	Cat# MA5-12387, RRID: AB_10980400
Rabbit anti-Phospho-Akt (Ser473) antibody	Cell Signaling Technology	Cat#4060, RRID:AB_2315049
Rabbit anti-Akt (pan) antibody	Cell Signaling Technology	Cat#4691, RRID:AB_915783
Rabbit anti-Phospho-PRAS40 (Thr246) antibody	Cell Signaling Technology	Cat#13175, RRID:AB_2798140
Rabbit anti- PRAS40 (D23C7) antibody	Cell Signaling Technology	Cat#2691, RRID:AB_2225033
Mouse anti-GAPDH antibody	Abcam	Cat#ab8245, RRID:AB_2107448
Alexa Fluor 488-AffiniPure Donkey Anti-Goat IgG (H + L)	Jackson ImmunoResearch Labs	Cat#705-545-147 RRID:AB_2336933
Cy3-AffiniPure Donkey Anti-Rabbit IgG (H + L)	Jackson ImmunoResearch Labs	Cat#711-165-152 RRID:AB_2307443
<b>Biological samples</b>		
Human primary glioblastoma	University Medical Center Schleswig-Holstein, Kiel	N/A
Human normal brain cortex tissue during traumatic brain injury surgery (non-malignant brain tissue)	University Medical Center Schleswig-Holstein, Kiel	N/A
Glioma intracranial xenografts	This study	N/A
Glioma subcutaneous xenografts	This study	N/A
Murine organotypic brain slices	This study	N/A
<b>Chemicals, peptides, and recombinant proteins</b>		
DMEM, high glucose, GlutaMAX(TM)	Gibco	Cat#10566016
FBS	Gibco	Cat# 10099141
Accutase solution	Sigma-Aldrich	Cat# A6964-100ML
EGF	Peptotech	Cat# 100-15
bFGF	Peptotech	Cat# 100-18B
Puromycin	Invivogen	Cat# ant-pr-1
Penicillin/Streptomycin	Gibco	Cat# 15140163
DMEM/F-12	Gibco	Cat# 11039-021
Insulin-Transferrin-Selenium (ITS -G) (100X)-10 mL	Thermo Fisher Scientific	Cat# 41400045
B-27 Supplement (50X), serum free-10 mL	Thermo Fisher Scientific	Cat# 17504001
N-2 Supplement (100X)-5 mL	Thermo Fisher Scientific	Cat#17502048
MEM Non-Essential Amino Acids Solution (100X)-100 mL	Thermo Fisher Scientific	Cat# 11140035
Monothioglycerol	Thermo Fisher Scientific	Cat# M1753-100ML
Human Insulin	PromoCell	Cat# C-52310

(Continued on next page)

<b>Continued</b>		
REAGENT or RESOURCE	SOURCE	IDENTIFIER
IL-34	Peprtech	Cat# 200-34-100UG
TGFβ1	Peprtech	Cat#100-21C-100UG
M-CSF	Peprtech	300-25-100UG
Recombinant Human CD200 (C-His)	BonOpus	BP004
CX3CL1	Peprtech	300-31-20 UG
Recombinant CCL18	R&D	Cat# 394-PA
CCL18 neutralizing antibody	Abcam	Cat# ab9849
CCR8 neutralizing antibody	R&D	Cat# MAB1249
Rabbit IgG Isotype Control	Abcam	Cat# ab171870
Rat IgG2B Isotype Control	R&D	Cat# MAB0061
Geltrex	Gibco	Cat#A14133-02
Thiazovivin, 1mg	Stem Cell Technologies	Cat#72252
Recombinant CCL5 (Rantes)	R&D	Cat#278-RN-010/CF
Recombinant IL-1beta	R&D	Cat#201-LB-005/CF
ReLeSR	Stem Cell Technologies	Cat#05872, Cat#05873
<b>Critical commercial assays</b>		
Brain Tumor Dissociation Kit	Miltenyi Biotech	Cat# 130-095-942
Stemdiff Hematopoietic Kit	Stemcell Technologies	Cat#5310
Cell Counting Kit-8	Dojindo	Cat#CK04
Proteome Profiler Human Phospho-Kinase Array Kit	R&D	Cat#ARY003C
CD11b (Microglia) MicroBeads, human and mouse	Miltenyi	Cat# 130-093-634
Human CCL18/PARC Quantikine ELISA Kit	R&D	Cat# DCL180B
<b>Deposited data</b>		
TCGA GBM RNA-seq datasets	Genomics Data Common	<a href="https://portal.gdc.cancer.gov/">https://portal.gdc.cancer.gov/</a> <a href="http://gliovis.bioinfo.cnio.es/">http://gliovis.bioinfo.cnio.es/</a>
Tumor Immune Estimation Resource (TIMER)	Genomics Data Common	<a href="http://timer.comp-genomics.org/">http://timer.comp-genomics.org/</a>
GEPIA 2	Genomics Data Common	<a href="http://gepia2.cancer-pku.cn/#index">http://gepia2.cancer-pku.cn/#index</a>
scRNA-seq data of glioma	<a href="#">Nefel et al. (2019)</a>	GEO: GSE131928
<b>Experimental models: Cell lines</b>		
HMGUi001-A	Helmholtz Zentrum München (HMGU)	<a href="https://hpscrg.eu/cell-line/HMGUi001-A">https://hpscrg.eu/cell-line/HMGUi001-A</a>
HMGUi001-A-10 (GFP iPSC line)	Berlin Institute of Health (BIH)	<a href="https://hpscrg.eu/cell-line/BIHi268-A-10">https://hpscrg.eu/cell-line/BIHi268-A-10</a>
U87MG	ECACC	NO. 89081402
U251MG	ECACC	NO. 89181493
LN229	ATCC	ATCC-CRL-2611
THP-1	ATCC	ATCC-TIB-202
293T	Gift from Dr. Shutao Pan obtained from ATCC	ATCC-CRL-3216
GBM1/20	This study	N/A
GBM12/19	This study	N/A
GBMa	This study	N/A
GBMb	This study	N/A
GBMc	This study	N/A
GBM1	This study	N/A
<b>Experimental models: Organisms/strains</b>		
BALB/c-Nude mice	GemPharmatech	Strain NO.D000521
CSF1R-EGFP C57BL6J mice	<a href="#">Sasmono and Williams (2012)</a>	N/A
C57BL6J mice	Max Delbrück Center	N/A
<b>Oligonucleotides</b>		
See <a href="#">Table S1</a> for oligonucleotide information		N/A

(Continued on next page)

**Continued**

REAGENT or RESOURCE	SOURCE	IDENTIFIER
<b>Recombinant DNA</b>		
psPAX2	Gift from Dr.Shutao Pan obtained from Addgene	Cat#12260
pMD2.G	Gift from Dr.Shutao Pan obtained from Addgene	Cat#12259
pGCSIL-001-shCCL18 with shRNA targeting sequence: sh#1, 5'-CAATAAGAAGTGGGTC CAGAA-3', sh#2, 5'-GCACAAGTTGGTACCA ACAAA-3'	GeneChem	N/A
pGCSIL-001-shCCR8 with shRNA targeting sequence: sh#1, 5'- GCGGAACCTTATTCAG ACAAAT -3', sh#2, 5'- GCAGCCAAATCTTC AACTACC -3'	GeneChem	N/A
pGCSIL-001-negative control with targeting sequence: 5'- CCTAAGGTTAAGTCGCCCTCG -3'	GeneChem	N/A
<b>Software and algorithms</b>		
Graphpad Prism 7.0	GraphPad Inc.	<a href="https://www.graphpad.com/">https://www.graphpad.com/</a>
ImageJ	NIH	<a href="https://imagej.nih.gov/ij">https://imagej.nih.gov/ij</a>
Tumor Immune Estimation Resource (TIMER)	<a href="#">Li et al. (2016)</a> <a href="#">Li et al. (2020)</a>	<a href="http://timer.comp-genomics.org/">http://timer.comp-genomics.org/</a>
IMARIS	Bitplane	<a href="https://imaris.oxinst.com/">https://imaris.oxinst.com/</a>
ZEN	Zeiss	<a href="https://www.zeiss.com/">https://www.zeiss.com/</a>

**RESOURCE AVAILABILITY**

**Lead contact**

Further information and requests for resources and reagents should be directed to and will be fulfilled by the Lead Contact Helmut Kettenman ([kettenmann@mdc-berlin.de](mailto:kettenmann@mdc-berlin.de)).

**Materials availability**

This study did not generate new unique reagents.

**Data and code availability**

- All data reported in this paper will be shared by the [lead contact](#) upon request.
- This study does not report original code.
- Any additional information required to reanalyze the data reported in the study is available from the [lead contact](#) upon request.

**EXPERIMENTAL MODEL AND SUBJECT DETAILS**

**Animals**

We used C57BL6J mice or MacGreen mice expressing EGFP under the control of the CSF-1R ([Sasmono and Williams, 2012](#)) on C57/BL6J background. Male mice (aged 14 days) were used for OBS experiments. The animals were handled according to the regulations and rules of Landesamt für Gesundheit und Soziales Berlin (LaGeSo) and Max Delbrück Center for Molecular Medicine, Berlin, Germany. Regarding the intracranial and subcutaneous brain tumor *in vivo* model, male BALB/c-Nude mice (6–8 weeks, weight 20–25 g, Strain NO.D000521) were obtained from GemPharmatech Co., Ltd (Jiangsu, China). These animals were handled according to the ethic approval of Tongji medical college, Huazhong University of Science and Technology, Wuhan, China. All littermates were randomly allocated to experimental groups.

**Human material**

All patients were operated at the Department of Neurosurgery, University Medical Center Schleswig-Holstein, Kiel. The study was approved by the Ethics Committee of the University of Kiel (approval no. D477/18) and was in accordance with the Helsinki Declaration of 1964 and its later amendments. Informed consent was obtained from all individual patients. Freshly resected tumor tissue was stored in DMEM at 4°C for <24 h until further experimental workup.

### Cell culture

Human glioma cell line U87MG (European Collection of Authenticated Cell Cultures, ECACC, No. 89081402), U251MG (ECACC, No. 89181493), LN229 (American Type Culture Collection, ATCC-CRL-2611) and human 293 T cells (Gift from Dr. Shutao Pan obtained from ATCC, ATCC-CRL-3216) were cultured in DMEM medium with supplements, 10% fetal calf serum (FCS), 50 units/mL penicillin, 50  $\mu$ g/mL streptomycin, and 200 mM glutamine (all purchased from Invitrogen, Darmstadt, Germany). THP-1 cells (American Type Culture Collection, ATCC, ATCC-TIB-202) were cultured in RPMI-1640 medium with 10% FCS, 50 units/mL penicillin, 50  $\mu$ g/mL streptomycin, 200 mM glutamine (Invitrogen) and 0.05 mM 2-Mercaptoethanol (Gibco-Thermo Fisher Scientific, Waltham, MA, USA). Prior to the experiment, THP-1 cells were treated with phorbol 12-myristate 13-acetate (PMA, 100 ng/mL) for 48 h. Glioma cell lines expressing the red fluorescence protein mCherry (U87MG-mCherry, U251MG-mCherry and LN229-mCherry cells) were generated according to our previous protocols (Buonfiglioli et al., 2019). Primary glioma cells were cultured from glioma resection. Briefly, tumor resections were first rinsed with PBS and dissociated using tumor dissociation kit (MiltenyiBiotec, Bergisch Gladbach, Germany). Cell suspension was then cultured in RPMI-1640 medium with 10% FCS, 50 units/mL penicillin, 50  $\mu$ g/mL streptomycin, 200 mM glutamine (Invitrogen) and 1% fibroblast growth factor (FGF, Peprotech Inc., Rocky Hill, United States)/epidermal growth factor (EGF, Peprotech Inc.). For blood monocyte derived macrophages, PBMCs were isolated from the healthy donors by Ficoll-Hypaque density gradient centrifugation. After washing, cells were then resuspended in Macrophage Serum Free (MSFM, Invitrogen) for 2 h incubation to remove non-adherent cells. The adherent cells were then incubated in DMEM +10% FBS +1% P/S + GlutaMAX (Gibco) supplemented with 10 ng/mL of human CSF1 (Peprotech) for 7 days and medium were changed every other day. hiPSC cells, HMGUi001-A (sex = female), were obtained from Helmholtz Zentrum München (HMGU). GFP labeled hiPSC cells, HMGUi001-A-10 were generated by Stem Cell Core Facility of Max Delbrück Center for Molecular Medicine.

### METHOD DETAILS

#### Bioinformatic analysis of TCGA GBM data and GEO dataset

For gene expression and survival estimation analysis, datasets including TCGA GBM RNA-seq, HU-133A, Agilent 4502 were processed via online GBM RNA-seq analysis platform GLIOVIS (<http://gliovis.bioinfo.cnio.es/>) (Bowman et al., 2017) and GEPIA (<http://gepia2.cancer-pku.cn/>) (Tang et al., 2019). For correlation evaluation between GAMs infiltration level and gene expression, TCGA GBM RNA-seq datasets were processed via TIMER platform (<http://timer.comp-genomics.org/>) (Li et al., 2020).

#### In vitro differentiation of iMGL

A pure iMGL culture was generated using previously published protocol (McQuade et al., 2018) with minor modifications. Briefly, HMGUi001-A or HMGUi001-A-10 (GFP iPSC line) hiPSC clusters were seeded onto a Geltrex-coated vessel into fresh E8 Home medium. On Day 0 wells containing approximately 50 clusters (per well of a 6-well plate) were selected. Hematopoietic progenitor cells (HPC) were generated using the STEMdiff™ Hematopoietic Kit (Stemcell Technologies, Vancouver, Canada). Therefore, on Day 0 2 mL Medium A were added to the selected well for mesodermal differentiation. On Day 2 1 mL of conditioned medium was carefully removed and replaced with 1 mL of fresh Medium A. On Day 3 Medium A was aspirated and 2 mL Medium B added to the well. 1 mL of Medium B was supplemented every other day. HPC were harvested by carefully removing the supernatant on days 10 and 12. HPC were replated into serum-free differentiation medium supplemented with IL-34 (100 ng/mL), M-CSF (25 ng/mL), TGF- $\beta$ 1 (50 ng/mL) at a density of  $1.3 \times 10^5$  HPC per well. 1 mL of fresh differentiation medium including the three supplements was added every other day until day 24. On day 24 medium was transferred leaving 3 mL conditioned medium behind, centrifuged at 300 g, 5 min before the supernatant was aspirated and the pellet resuspended in 1 mL of fresh differentiation medium before being added back to the well. Again, the culture was supplemented with 1 mL of fresh differentiation medium including the three supplements every other day until day 37. Similar to day 24 medium, except for 3 mL that were again left behind, was transferred and centrifuged at 300 g, 5 min on day 37 and the pellet resuspended in differentiation medium now including an additional 100 ng/mL of CD200 and 100 ng/mL of CX3CL1. Again, on day 39 1 mL of fresh medium containing the five supplements was added. iMGL were ready to be harvested on day 40 or kept in culture for up to a week.

#### Human GAM isolation by magnetic activated cell sorting (MACS)

GAMs were freshly isolated by MACS as previously described (Huang et al., 2020). Briefly, after washing with PBS, tumor tissue from human glioma samples or ex-vivo slices was enzymatically digested into a single-cell-suspension using Adult Brain Dissociation Kit™ (MiltenyiBiotec). The tissue was further dissociated, and debris was removed by applying a 40  $\mu$ m cell strainer (MiltenyiBiotec). Next, the cell suspension was incubated with CD11b microbeads™ in MACS buffer (PBS supplemented with 0.5% BSA and 2 mM EDTA) for 15 min. Cells were then loaded onto a MACS column (MiltenyiBiotec), after washing the column with MACS buffer. CD11b-positive and CD11b-negative cells were eluted from the column. A fraction of the isolated cells was stained with CD11b antibody for FACS analysis to verify cell purity. Populations of CD11b-positive and negative cells were used for investigating gene expression changes by real-time quantitative PCR.

### Small interfering RNA (siRNA) and short hairpin RNA (shRNA) mediated genes knockdown

The sequences of siRNA targeting CCR8: si#1, sense 5'-AUUUGUCUGAAUAAGUCCGC-3', antisense 5'-GGAACUUAUUCAGACAAAUGG-3'; si#2, sense 5'-AUGUUCAUUUUGAAGUUGGUG-3', antisense 5'-CCAACUUCAAAAUGAACAUUUU-3'; ACP5: si#1, sense 5'-AUCAGUAAACAGAAAGAUGCUU-3', antisense 5'-GCAUCUUUCUGUUACUGAUGU-3'; si#2, sense 5'-AGAAAGAUGCUU GAUUUAGGA-3', antisense 5'-CUAAAUCAAGCAUCUUUCUGU-3'; PITPNM3: si#1, 5'-GAACTGTACCGGGTTTCCTTGAGAA-3', si#2, CATCTGCTCTGAGGCTTCTCGCTT-3'. The negative control siRNA were obtained from Thermofisher Scientific (siRNA Negative Control). For siRNA mediated CCR8, ACP5 and PITPNM3 knockdown, cells were transfected with siRNA using Lipofectamin 3000 (Thermofisher Scientific) according to the manufactrue instructions.

For CCL18 shRNA and CCR8 shRNA, target sequences were: CCL18: sh#1, 5'-CAATAAGAAGTGGGTCCAGAA-3', sh#2, 5'-GCA CAAGTTGGTACCAACAAA-3'; CCR8: sh#1, 5'-GCGGAACTTATTTCAGACAAAT-3', sh#2, 5'-GCAGCCAAATCTTCACTACC-3'. Negative control: 5'-CCTAAGGTTAAGTCGCCCTCG-3'. The shRNA expression plasmids were ordered and constructed from GeneChem (Shanghai Genechem Co.,Ltd., Shanghai, China). Regarding transfection, shRNA expression plasmids together with packaging plasmids (psPAX2 and pMD2.G, Gift from Dr. Shutao Pan obtained from Addgene, Cat#12260 and Cat#12259) were transfected into 293 T cells (at 50% confluence) using Lipofectamin 3000 (Thermofisher Scientific) and P3000 reagent (Thermofisher Scientific) according to the manufacturers instructions. After transfection, medium was changed at 6 h and 24 h. Supernatant of the cells was collected and filtered using 0.22  $\mu$ m filter at 72 h after transfection. Glioma cell lines or THP-1 cells were infected with the supernatant for 3 days in the presence of 10  $\mu$ g/mL Polybrene (Yeason, Shanghai, China, Cat# 40804ES76). Puromycin (1  $\mu$ g/mL) was used for 7 days to select cells after infection.

### Organotypic brain slice (OBS) model and tumor inoculation

OBS were prepared as described previously (Markovic et al., 2009). Briefly, 14-day-old WT or MacGreen mice were decapitated, and brains were cut in coronal plane into 250  $\mu$ m sections with a vibratome (Leica VT1000S, Wetzlar, Germany). Brain slices were collected with a sterile plastic pipette (7 mm diameter) and transferred onto cell culture inserts with 0.4  $\mu$ m pores (Becton Dickinson, Franklin Lakes, USA), which were fitted into wells of a 6-well-plate. 1 mL culture medium containing DMEM supplemented with 10% heat inactivated FCS, 0.2 mM glutamine, 100 U/mL penicillin, and 100 mg/mL streptomycin was added into each well and after overnight incubation medium was changed with cultivation medium containing 25% heat-inactivated FCS, 25% Hank's balanced salt solution, 50% DMEM and 50 mM sodium bicarbonate, 2% glutamine, 250 ng/mL insulin (Invitrogen), 2.46 mg/mL glucose (Braun Melsungen, Melsungen, Germany), 0.8 mg/mL vitamin C (Sigma-Aldrich), 25 U/mL penicillin, 100 mg/mL streptomycin, and 5 mM Tris (all from Invitrogen). To deplete microglia in OBS, liposome-encapsulated clodronate diluted with culture medium (1:10) was added into the well while liposome-encapsulated PBS served as a control. After 48 h incubation, medium containing liposomes was replaced by cultivation medium and incubated for another 48 h. Afterward, 5000 U87MG-mCherry, U251MG-mCherry, LN229-mCherry or primary glioma cells which were labeled with DiD dye (Thermofisher) together with or without 5000 iMGL or THP-1 cells were slowly injected into the caudate putamen region of the slice in 150  $\mu$ m depth of both hemispheres. After 5 d, slices were washed and fixed with 4% PFA. Tumor volumes and area were measured by confocal microscopy (LSM700, Zeiss, Oberkochen, Germany) with z stack scanning and were 3D reconstructed by IMARIS software (Bitplane, Zurich, Switzerland) to determine tumor volume. For treatment, recombinant CCL18 (R&D, Minneapolis, USA), normal goat IgG control (Isotype, R&D), CCL18 neutralizing antibody (aCCL18, R&D), CCR8 neutralizing antibody (aCCR8, R&D) or Rat IgG2B Isotype Control (Isotype, R&D) were applied to the medium after tumor implantation, and every other day, fresh recombinant protein, antibody, or isotype were added during medium change.

For iMGL/THP-1 cells isolation from organotypic brain slices 5 days after tumor inoculation, we harvested the tumor tissue with a scalpel and transferred it into 1.5 mL Eppendorf tubes. For control microglia, cells were similarly collected from non-tumor slices. Then the tissues were enzymatically digested to obtain a single-cell-suspension using Adult Brain Dissociation Kit<sup>TM</sup> (MiltenyiBiotec) followed by the microglia isolation procedure by MACS as described above.

### CCK-8 counting kit and scratch (wound healing) assay

Supernatant from the glioma cells or organotypic brain slices were collected into 96-well-plate CCK-8 reagent (Dojindo, Osaka, Japan) was added (10  $\mu$ l per well) into the wells containing supernatant in 96-well-plate and incubated for 2 h. Plates were measured with a multi-reader at 450 nm absorbance. Results were normalized to the absorbance of the control group.

For scratch assay, 4  $\times$  10<sup>5</sup> fluorescence labeled glioma cells were seeded per well to a 2 cm<sup>2</sup> round culture dish for growing to confluence. A single scratch was made by sterile pipette tip under the center of the wells. Phosphate-buffered saline (PBS) was used to wash away cell debris and floating cells. Cells were then incubated in the serum free DMEM with or without recombinant CCL18 treatment (10 or 100 ng/mL) for 24 h. Image were taken under fluorescence microscope. Area of non-invading are assessed by ImageJ software.

### Transwell assay and colony formation assay

Glioma cells were harvested and resuspended in serum-free DMEM (Invitrogen). The Corning 8- $\mu$ m Transwell chamber (Corning Inc., New York, USA) was placed on the 6-well plate (Corning Inc.). The lower chamber was filled with DMEM with 10% FCS, and the same amount of medium with the 10000 glioma cells was added to the upper chamber. 100 ng/mL recombinant CCL18

(R&D) was applied into both upper and lower chamber. After culturing for 12 h at 37°C and 5% CO<sub>2</sub>, the cells were then fixed with methanol and stained with crystal violet. Migrated cells were quantified by counting 5 random fields under the microscope (Olympus).

For colony formation assay, 500 glioma cells were seeded in the 6-well plate (Corning Inc.) and recombinant CCL18 (100 ng/mL) was added to the medium. Medium with recombinant CCL18 was changed every 3 days. After 14 days, cells were fixed with methanol and stained with crystal violet. The colonies of each well were counted.

### Glioma xenografts

The intracranial model were generated as previously described (Hu et al., 2015). Briefly, male 6–8 week-old BALB/c nude mice were randomly assigned and intraperitoneal injection of ketamine (0.1 mg/g) and xylazine (0.02 mg/g). Head of the animals were fixed on the a stereotactic head frame and a burr hole was made 1.5 mm right of the midline and 1 mm anterior to the bregma. The 0.5 μL of PBS containing 2 × 10<sup>4</sup> U87MG or U251MG glioma cells (WT or vector or shRNA transfected) were then inoculated at 3 mm depth from dura with a 1 μL-Hamilton microsyringe. After tumor implantation, the tumor bearing mice were kept under pathogen-free conditions. Neurological signs as well as body weight were monitored daily. For recombinant CCL18 treatment, 10 ng or 100 ng recombinant CCL18 (R&D) were injected into the same place as tumor inoculation on 7 and 14 days after tumor implantation. For CCR8 blockade, 1 μg of CCR8 neutralizing antibody (R&D) was intraperitoneal applied to the tumor bearing animals every other day after tumor inoculation.

Regarding subcutaneous glioma *in vivo* xenografts, male 6-8 week-old BALB/c nude mice were randomly assigned and anesthetized. Glioma cells together with THP-1 macrophages (WT, vector or shRNA transfected) were subcutaneously co-injected (with 1:1 ratio) into right flank of the mice. Tumor volumes were then evaluated every 3 days and calculated according to the formula,  $V \text{ (mm}^3\text{)} = 1/2 \text{ (L} \times \text{W}^2\text{)}$ .

### Immunofluorescent staining

Immunofluorescence staining and image processing were performed according to previous protocols (Huang et al., 2020). Human glioma specimens were prepared following the procedure previously described (Vinnakota et al., 2013). Slices were washed 3 times with PBS for 5 min and blocked with 5% of donkey serum and 0.1% Triton-X (Sigma-Aldrich). Human tumor slice staining was performed by adding primary antibodies overnight at 1:400 for Iba-1, 1:100 for CCL18, 1:200 for CCR8 and 1:200 for ACP5 (all from Abcam, Cambridge, United Kingdom). For OBS staining, slices were incubated with primary antibodies on a shaker at 4°C overnight. Primary antibodies were goat anti-Iba1 (Abcam, Cambridge, UK) 1:400 and rabbit anti-P2Y12 (Genetex, CA, United States) 1:200 or rabbit anti-TMEM119 (Invitrogen) 1:100. As secondary antibody, Cy3 conjugated goat anti-rabbit IgG (1:200; Jackson ImmunoResearch Laboratories, West Grove, United States) or Alexa Fluor 488 conjugated anti-goat or anti-mouse antibodies (1:200; Jackson ImmunoResearch Laboratories) were used. Nuclei were counterstained with 4,6-diamidino-2-phenylindole (DAPI, Sigma-Aldrich). Images were taken using a confocal microscope (LSM700, Zeiss) with 20x or 40x oil objectives. Morphology including sphericity and cell body volume of the iMGL on OBS was analyzed by IMARIS software (Bitplane) using surface module.

### Real-time quantitative PCR (qPCR)

Total RNA was isolated using Promega RNA mini kit (Promega, Wisconsin, United States) according to the manufacturer's instructions. Quality and yield were determined by NanoDrop 1000 (PeqLabBiotechnologie). cDNA was synthesized using 100 ng total RNA with SuperScript II reverse transcriptase kit (Invitrogen). RT-PCR gene amplification was performed in duplicate using SYBR Green PCR mix (Applied Biosystems) and 7500 Fast Real-Time PCR System (Applied Biosystems). Primer sequences generated by Biotex (Berlin, Germany) were listed as follows: Chemokine (C-C motif) ligand 5 (CCL5: sense 5'-CCAGCAGTCGCTTTGTCAC-3', antisense 5'-CTCTGGGTTGGCACACACTT-3'), Osteopontin (OPN: sense 5'-GAAGTTTCGACACCTGACAT-3', antisense 5'-GTATGCACCAT TCAACTCCTCG-3'), Chemokine (C-C motif) ligand 18 (CCL18: sense 5'-AGCTCTGCTGCCTCGTCTAT-3', antisense 5'-GGCCTCTC TTGGTTAGGAGG-3'), matrix metalloproteinase 14 (MMP14: sense 5'-GGTACAGCAATATGGCTACC-3', antisense 5'-GATGGCCGC TGAGAGTGAC-3'), vascular endothelial growth factor (VEGF: sense 5'-AGGGCAGAATCATCACGAAGT-3', antisense 5'-AGGGTCTCG ATTGGATGGCA-3'), TATA-binding protein (TBP: sense 5'-AGCGCAAGGGTTTCTGGTTT-3', antisense 5'-CTGAATAGGCTGTG GGGTCA-3'), arginase 1 (ARG1: sense 5'-TGGACAGACTAGGAATTGGCA-3', antisense 5'-CCAGTCCGTC AACATCAAACT-3'), Interleukin 10 (IL10: sense 5'-GACTTTAAGGGTTACCTGGGTTG-3', antisense 5'-TCACATGCGCCTTGATGTCTG-3'), transforming growth factor beta (TGFbeta: sense 5'-CAATTCCTGGCGATACCTCAG-3', antisense 5'-GCACAACCTCCGGTGACATCAA-3'), acid phosphatase 5 (ACP5, sense 5'-GACTGTGCAGATCCTGGGTG-3', antisense 5'-GGTCAGAGAATACGTCCTCAAAG-3'), C-C motif chemokine receptor 8 (CCR8: sense 5'-CTCACTGCTGTGTGAACCCT-3', antisense 5'-CACAGCTCTCCCTAGGCATT-3'). The results were analyzed by 2-ΔΔCT ways normalized to tpb and were presented as fold change normalized to control group.

### Enzyme linked immunosorbent assay (ELISA)

The supernatant from blood monocyte derived macrophages (ctrl MAC), GAMs isolated from patients derived GBM using MACS, blood monocyte derived macrophages after co-culturing with glioma cells were collected and stored in -80°C freezer. CCL18 protein levels in the supernatant were then determined with CCL18 ELISA kit (R&D systems, Cat# DCL180B) according to manufacturer's instructions.

### Western blot

Whole-cell protein extracts were prepared from U87MG, U251MG, or LN229 glioma cells using RIPA lysis buffer (Sigma Millipore) containing EDTA-free protease inhibitor cocktail tablets (Roche Diagnostics). Protein concentration was determined by a BCA protein assay kit (Thermo Fisher Scientific), and 20  $\mu$ g of total protein of each sample was resolved on a 10% SDS-PAGE gel, followed by wet transfer of resolved proteins onto a PVDF membrane (GE Healthcare). Membranes were blocked and followed by overnight incubation at 4°C with rabbit anti-phosphorylated PRAS40 (1:500), rabbit total-PRAS40 (1:500), rabbit anti-phosphorylated-Akt (Ser473) (1:500), anti-total-Akt antibodies (1:500) (all from CST) or mouse anti-GAPDH (1:2000) (Abcam). Membranes were incubated with a secondary anti-rabbit HRP antibody (1:2000; Thermo Fisher Scientific), developed with SuperSignal West Pico Chemiluminescence substrate kit (Thermo Fisher Scientific). Signal was detected by GeneGnome XRQ Chemiluminescence Imaging System (GeneGnome XRQ; Syngene) exposure instrument. Gray intensity of the bands was analyzed using ImageJ 1.8.0 software (NIH, United States). The relative expression levels of the proteins were standardized by densitometric analysis to total-Akt, total-PRAS 40 or GAPDH levels, respectively.

### Proteome profiler™ human phospho-kinase array

Detection of the protein phosphorylation was carried out according to the Proteome Profiler™ Human Phospho-Kinase Array Kit manual. In short, LN229 cells were treated with rCCL18 for 48 h to later isolate the protein with RIPA buffer. Human Phospho-Kinase Array membranes A and B were incubated in Array Buffer 1 for 1 h on a rocking platform. Then, each membrane was incubated with 600  $\mu$ L of LN229 protein lysate at 4°C overnight. On the following day the membranes were washed 3  $\times$  10 min with Wash Buffer. Next, membrane A and membrane B were placed in diluted Detection Antibody Cocktail A and B respectively for 2 h in RT on a rocking platform. Afterward, they were washed 3  $\times$  10 min with Wash Buffer and incubated in Streptavidin-HRP diluted in Array Buffer2/3 for 30 min in room temperature. Then the 3  $\times$  10 min wash in Wash Buffer was repeated. As the final step the membranes were covered with Chemi Reagent Mix and the chemiluminescence was immediately detected with the LI-COR Odyssey Fc imaging system.

### QUANTIFICATION AND STATISTICAL ANALYSIS

All data are represented as mean  $\pm$  SD. Datasets were analyzed statistically by Graphpad Prism7.0 software (Graphpad, San Diego, USA). Specifically, the one-way ANOVA with Tukey's post-hoc comparison test or unpaired two tailed Student's t-test was used to compare the differences of OBS tumor volume (fold changes) as stated in the figure legends. For RT-qPCR results, paired or unpaired two tailed Student's t-test or one-way ANOVA with Tukey's post-hoc comparison test was used as described in the figure legends. For quantification of Westernblot intensity, difference among multiple groups were compared using one-way ANOVA with Tukey's post-hoc comparison test. For proliferation assay and migration assay, one-way ANOVA with Tukey's post-hoc comparison test was used as stated in the figure legend. Percent survival of mice with tumors was analyzed by the Log rank (Mantel-Cox) test. The  $p < 0.05$  is interpreted as statistically significant and the specific meaning of the asterisk is listed as: \* =  $p < 0.05$ , \*\* =  $p < 0.01$ , \*\*\* =  $p < 0.001$  and \*\*\*\* =  $p < 0.0001$ .